Chapter 3

# Physicochemical Properties of Chlorophylls in Oxygenic Photosynthesis — Succession of Co-Factors from Anoxygenic to Oxygenic Photosynthesis

Masami Kobayashi, Shinya Akutsu, Daiki Fujinuma, Hayato Furukawa, Hirohisa Komatsu, Yuichi Hotota, Yuki Kato, Yoshinori Kuroiwa, Tadashi Watanabe, Mayumi Ohnishi-Kameyama, Hiroshi Ono, Satoshi Ohkubo and Hideaki Miyashita

Additional information is available at the end of the chapter

http://dx.doi.org/10.5772/55460

## 1. Introduction

Chlorophylls are essential components in oxygenic photosynthesis, and chlorophyll (Chl) *a* (Fig. 1) is the major chlorophyll in cyanobacteria, algae and terrestrial plants. However, primary charge separation is initiated by a few specially-tailored chlorophylls in the reaction centers (RCs). Excitation of the primary donor reduces the primary and secondary electron acceptors, which again are often specially-tailored chlorophylls; *e.g.*, the $13^2$-epimer of Chl *a,* Chl *a'* (Fig. 1), constitutes the primary electron donor of P700 in PS I as a heterodimer of Chl *a*/*a'* (Kobayashi et al. 1988; Jordan et al. 2001), and a metal-free Chl *a*, pheophytin (Phe) *a* (Fig. 1), functions as the primary electron acceptor in PS II (Klimov et al. 1977a,b; Zouni et al. 2001) (Fig. 2).

In 1996, a unique cyanobacterium, *Acaryochloris marina*, with Chl *d* as the dominant chlorophyll was discovered in colonial ascidians (Miyashita et al. 1996). Though P740 in PS I of *A. marina* is composed of Chl *d'*, pheophytin in PS II is not *d*-type but *a*-type (Akiyama et al. 2001). One of the difficulties in finding Chl *d* in nature was its overlap with Chl *b* on a reversed-phase HPLC trace. To make matters worse, Chl *d* had been thought to have a lower oxidation potential than Chl *a* even though no experimental evidence was available, mainly because a midpoint potential, $E_m$, for P740 in *A. marina* was shown to be +335 mV (Hu et al. 1998),

marvelously more negative than that for P700 (ca. +470 mV) in the Chl *a*-type cyanobacteria. The fact that the $Q_Y$-band of Chl *d* is at the longest wavelength compared with Chls *a* and *b* seems to have led to some misapprehensions concerning the oxidation potential of Chl *d*; one estimated that Chl *d* had the lowest oxidation potential among Chls *a*, *b* and *d*. In 2007, however, the $E_{ox}$ value of Chl *d in vitro* was first determined and found to be higher than that of Chl *a* (Kobayashi et al. 2007), and hence the $E_m$ of P740 was re-examined; the value was ca. + 435 mV (+430 mV: Benjamin et al. 2007, Telfer et al. 2007, and +439 mV: Tomo et al. 2008), being far positive of the initial report (+335 mV) and almost equal to the Chl *a*-type P700 values, around +470 mV (Brettel 1997, Krabben et al. 2000, Ke 2001, Itoh et al. 2001, Nakamura et al. 2004) (see Fig. 7 in Ohashi et al. 2008).

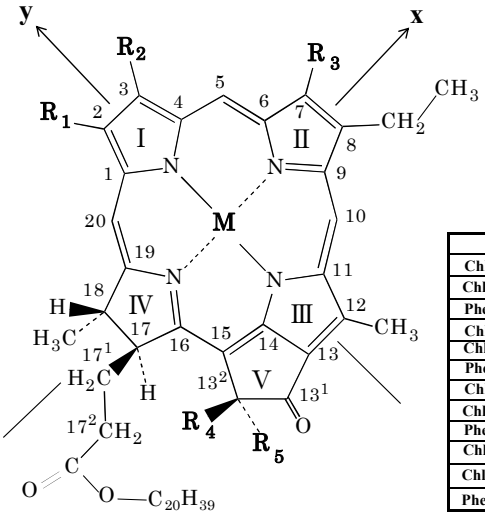


| | M | $R_1$ | $R_2$ | $R_3$ | $R_4$ | $R_5$ |
|---|---|---|---|---|---|---|
| Chl *a* | Mg | $CH_3$ | $CH{=}CH_2$ | $CH_3$ | H | $COOCH_3$ |
| Chl *a'* | Mg | $CH_3$ | $CH{=}CH_2$ | $CH_3$ | $COOCH_3$ | H |
| Phe *a* | 2H | $CH_3$ | $CH{=}CH_2$ | $CH_3$ | H | $COOCH_3$ |
| Chl *b* | Mg | $CH_3$ | $CH{=}CH_2$ | CHO | H | $COOCH_3$ |
| Chl *b'* | Mg | $CH_3$ | $CH{=}CH_2$ | CHO | $COOCH_3$ | H |
| Phe *b* | 2H | $CH_3$ | $CH{=}CH_2$ | CHO | H | $COOCH_3$ |
| Chl *d* | Mg | $CH_3$ | CHO | $CH_3$ | H | $COOCH_3$ |
| Chl *d'* | Mg | $CH_3$ | CHO | $CH_3$ | $COOCH_3$ | H |
| Phe *d* | 2H | $CH_3$ | CHO | $CH_3$ | H | $COOCH_3$ |
| Chl *f* | Mg | CHO | $CH{=}CH_2$ | $CH_3$ | H | $COOCH_3$ |
| Chl *f'* | Mg | CHO | $CH{=}CH_2$ | $CH_3$ | $COOCH_3$ | H |
| Phe *f* | 2H | CHO | $CH{=}CH_2$ | $CH_3$ | H | $COOCH_3$ |

**Figure 1.** Molecular structure and carbon numbering of chlorophylls, according to the IUPAC numbering system. Naturally occurring chlorophylls are designated by squares.

In 2010, a red-shifted chlorophyll was discovered in a methanolic extract of Shark Bay stromatolites, and was named Chl *f* (Chen et al. 2010); a Chl *f*-containing filamentous cyanobacterium was purified and named as *Halomicronema hongdechloris* (Chen et al. 2012). In 2011, a Chl *f*-like pigment was discovered in a unicellular cyanobacterium, strain KC1, isolated from Lake Biwa (Ohkubo et al. 2011), but there were also difficulties in its identification because there were not systematic physicochemical data as to Chls *a*, *b*, *d* and *f* acquired under the same conditions. For example, the optical peak wavelengths of the red-shifted chlorophyll purified from the strain KC1 in methanol are almost the same as the reported values of Chl *f* ($\lambda$ = 406 nm and 706 nm), while the reported ratio of Soret/$Q_Y$-bands exhibited a large difference; the pigment purified from KC1 showed 0.9, but the reported ratio for Chl *f* was surprisingly high, 1.9. What is worse, the $^1$H-NMR chemical shifts of formyl-H of Chl *b* and *f* in acetone $d_6$ at 263 K being presented in this chapter are 11.31 and 11.22, respectively, but the corresponding

http://dx.doi.org/10.5772/55460

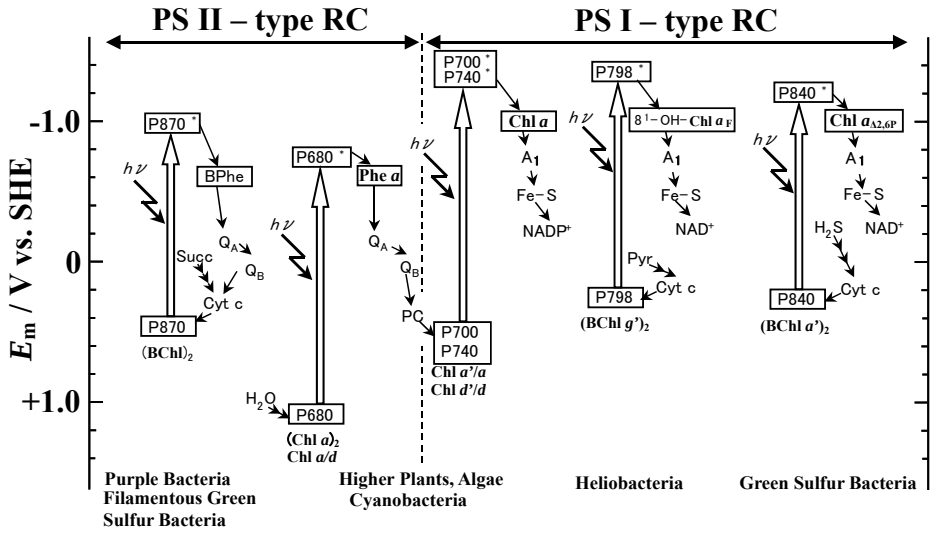


**Figure 2.** Schematic comparison of photosynthetic electron transport in PS I-type RC and PS II-type RC. Components are placed according to their estimated or approximate midpoint potentials. The arrows indicate the direction of electron flow. In order to simplify the figure, some primary electron donors, P970, P850 and P865 are omitted here: P970 and P850 are the primary electron donors of BChl *b* and Zn-BChl *a* containing purple bacteria, respectively; P865 is the primary electron donor of green filamentous bacteria. Figure adapted from Akutsu et al. (2011).

values reported were 11.22 for Chl *b* in $CDCl_3$ at unknown temperature and 11.35 for Chl *f* in $CD_2Cl_2/d_5$-pyridine(97/3, *v*/*v*) at 293 K, respectively, where our data are directly counter to the reported pair. These facts exhibit that chemical shift is highly sensitive to both solvents and temperature.

In this chapter, we present systematic and essential physicochemical properties of chlorophylls *in vitro* obtained under as common conditions as possible, introducing the detailed experimental procedures; HPLC, absorption, circular dichroism, mass, NMR and redox potential. We also introduce the succession of co-factors in PS I RCs from the viewpoints of minor but key chlorophylls (Fig. 3). In the future, our basic data will help researchers to identify the molecular structures of newly discovered chlorophylls and determine and/or predict their characteristics.

## 2. Chlorophylls in oxygenic photosynthesis

### 2.1. Popular chlorophylls: Chlorophylls *a* and *b*

In 1818, the term chlorophyll (Chl), the green (Greek *chloros*) of leaf (Greek *phyllon*), was introduced for the pigments extracted from leaves with organic solvents (Pelletier and Caventou 1818). In 1903, a Russian botanist Tsvet(Tswett) (in Russian meaning "colour") separated leaf pigments by chromatography (from Greek *chroma* and *graphein* meaning "color"

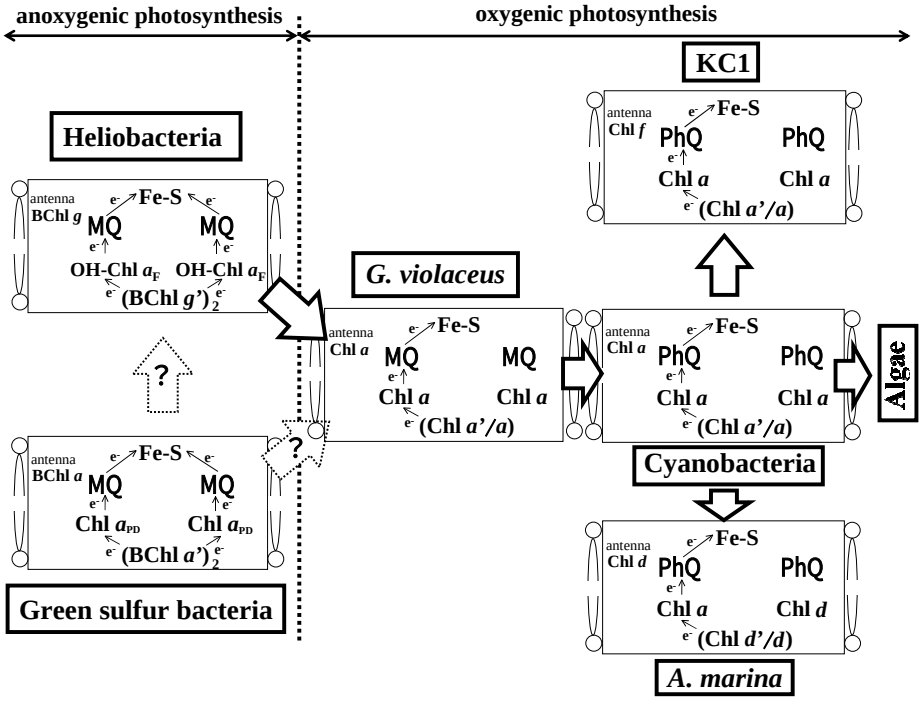


**Figure 3.** Schematic arrangement of co-factors in the PS I-type RCs. Our hypothesis about the evolution of the PS I-type RCs from the viewpoint of the molecular modifications of chlorophylls and quinones are designated by solid arrows.

and "to write", respectively) into the blue Chl *a*, the green Chl *b* and several yellow to orange carotenoids.

### 2.2. Recently discovered chlorophylls in algae

#### *2.2.1. Chlorophyll d in a cyanobacterium, Acaryochloris marina*

In 1943, Chl *d* (Fig. 1) was first reported as a minor pigment in several red macroalgae (Manning and Strain 1943). In 1996, a unique cyanobacterium, *Acaryochloris marina*, was isolated from colonial ascidians containing Chl *d* as the dominant chlorophyll (Miyashita et al. 1996; see Introduction in a review by Ohashi et al. 2008 for the short history of Chl *d* discovery).

#### *2.2.2. Chlorophyll f in a cyanobacterium, strain KC1, isolated from Lake Biwa*

A Chl *f*-producing cyanobacterium, strain KC1, was discovered by Miyashita, one of the authors of this chapter. The discovery story was a kind of fortunate accident, similar to that of Chl *d*-producing cyanobacterium, *A. marina* (Miyashita et al. 1996, Ohashi et al. 2008). Strain KC1 was a by-product during the hunting of chlorophyll *d*-producing

http://dx.doi.org/10.5772/55460

cyanobacteria in freshwater environment. Chl *d* had been only produced by cyanobacteria in the genus *Acaryochloris*, and the strains in *Acaryochloris* had been isolated only from saline environments such as the marine or salty lake but not from freshwater environments at all (Murakami et al. 2004, Miller et al. 2005, Mohr et al. 2010, Behrendt et al. 2011). Moreover, the strain *A. marina* MBIC11017 dose not grow in freshwater media and requires sodium chloride for its growth at more than 1.5% (*w*/*v*) in the medium (Miyashita et al. 1997). Chlorophyll *d* was, however, detected in the sediment at the bottom of Lake Biwa, the largest freshwater lake in Japan (Kashiyama et al. 2008), bringing us the idea that Chl *d*-containing algae exist in this lake. We collected algal mats and lake water from a shore zone of Lake Biwa at 24th, Apr. 2008. The samples were suspended in several media for freshwater algae, diluted and dispensed into cell culture plate or on agar plates. Those culture/agar plates were kept in an incubator with near infrared (NIR) light as the sole light source, because we expected that a Chl *d*-containing alga should grow faster than other algae under such light condition. Colony of *Acaryochloris* cells grown under NIR light looked yellow-green rather than blue-green of common cyanobacteria, and we also saw several yellow-green colonies (Oct. 2008). Our attempt to isolate a Chl *d*-containing freshwater *Acaryochloris* sp. from Lake Biwa turned out to be a success (Feb. 2010) (details will be reported elsewhere). Miyashita checked the culture/agar plates, which were left for a long time in the incubator under NIR light, and some unusual cyanobacterial colonies were found (Oct. 2009). The colonies were different from that of *Acaryochloris* sp. in color; being dark-blue-green rather than yellow-green. The cells grew under NIR light as the sole light source when we put them in a freshwater medium. Morphological features of the cells were similar to those of *Acaryochloris* sp. in that the cell was unicellular, spherical to subspherical and aggregated. We expected that the organism was a new Chl *d*-containing cyanobacterium which was closely related to the genus *Acaryochloris*, phylogenetically. The results of HPLC analysis disappointed us, since the cyanobacterium possessed no Chl *d* at all, and Chl *a* as the major chlorophyll like common cyanobacteria. Immediately thereafter, however, came an excitement when an unusual chlorophyll was detected (22nd. Jan. 2010). The pigment showed typical two absorption peaks in the Soret (406 nm) and $Q_Y$ (707 nm) regions in MeOH; they were clearly different from those of known chlorophylls. We concluded that the pigment was a new chlorophyll that should be named "Chl *f* ". We started mass culture of the cells for chemical characterization such as detailed spectral properties, molecular mass and chemical structure. At around the same time, Chen et al. (2010) reported the discovery of Chl *f* in a methanolic extract of Shark Bay stromatolites incubated under NIR light for the initial purpose of the isolation of new Chl *d*-containing phototrophs. Discoveries are mostly accidental.

Note that in the strain KC1 Chl *f* was not induced under white fluorescent light even if NIR LED was also used as additional light. Further, neither Chl *f*′ nor Phe *f* was detected, suggesting that Chl *a*′ and Phe *a* function as P700 and the primary electron acceptor in PS II, respectively, as in common cyanobacteria (Akutsu et al. 2011). The results indicate that Chl *f* may function as not an electron transfer component but an antenna part. Chl *f* is not the major photopigment, and may function as an accessory chlorophyll, although the function of Chl *f* in energy storage

is under debate, because uphill energy transfer is needed to deliver the excitation energy to Chl *a* molecules in the RC (Chen and Blankenship 2011).

### 2.3. Specially-tailored chlorophylls associated with reaction centers

#### *2.3.1. Prime-type chlorophylls as the primary electron donors in PS I*

##### *2.3.1.1. Chlorophyll a′ and P700*

The $13^2$-epimer of Chl *a*, Chl *a′* ("*a*-prime") (Fig. 1), was first reported in 1942 (Strain and Manning 1942). In 1988, it was proposed that Chl *a′* constitutes P700 as a heterodimer of Chl *a*/*a′* (Fig. 2) (Kobayashi et al. 1988), and the idea has been confirmed in 2001 (Jordan et al. 2001). As seen in Fig. 2, it has also been shown that P798 consists of BChl *g′* in the RC of heliobacteria in 1991 (Kobayashi et al. 1991), and that P840 consists of BChl *a′* in green sulfur bacteria in 1992 (Kobayashi et al. 1992, 2000), suggesting that prime-type chlorophylls are essential as the primary electron donors in the PS I-type RCs (see Figs. 2 and 3). For more details, see Chapter 4 in Kobayashi et al. (2006).

##### *2.3.1.2. Chlorophyll d′ and P740 in Acaryochloris marina*

Chl *d′*, the $13^2$-epimer of Chl *d* (Fig. 1), was always detected in *A. marina* as a minor component, while Chl *a′* was absent (see Fig. 6(C)) (Akiyama et al. 2001). P740, the primary electron donor of PS I in *A. marina*, was initially proposed to be a homodimer of Chl *d* (Hu et al. 1998), then a homodimer of Chl *d′* (Akiyama et al. 2001), and finally a Chl *d*/*d′* heterodimer (Fig. 2) (Akiyama et al. 2002, 2004; Kobayashi et al. 2005, 2007: Ohashi et al. 2008), just like the Chl *a*/*a′* for P700 in other cyanobacteria and higher plants (Figs. 2 and 3): a dimer model for P740 was supported by FTIR spectroscopy (Sivakumar et al. 2003). The finding of Chl *d′* in *A. marina* appears to ensure our hypothesis that prime-type chlorophyll is a general feature of the primary electron donor in the PS I-type RCs (see Figs. 2 and 3). The homology of PsaA and PsaB between *A. marina* and other cyanobacteria is low (Swingley et al. 2008), which may reflect the replacement of Chl *a* by Chl *d*, also Chl *a′* by Chl *d′*, in the PS I RC of *A. marina* (see Fig. 3).

It is interesting to note that the primary electron acceptor, $A_{0'}$ in PS I of *A. marina* is not Chl *d* but Chl *a* (Figs. 2 and 3), which was first shown by laser photolysis experiment (Kumazaki et al. 2002), and then supported by flash-induced spectral analysis (Itoh et al. 2007). The results support our hypothesis that Chl *a*-derivative is a general feature of $A_0$ in the PS I-type RCs (see Figs. 2 and 3).

##### *2.3.1.3. Evolutionary relationship between chlorophylls and PS-I type reaction centers*

Here we introduce our hypothesis about the evolution of the PS I-type RCs based on the structures of chlorophylls and quinones (Fig. 3). The prime-type chlorophylls, bacteriochlorophyll (BChl) *a′* in green sulfur bacteria, BChl *g′* in heliobacteria, Chl *a′* in Chl *a*-type PS I, and Chl *d′* in Chl *d*-type PS I, function as the special pairs, either as homodimers, (BChl *a′*)$_2$ and (BChl *g′*)$_2$ in anoxygenic organisms, or heterodimers, Chl *a*/*a′* and Chl *d*/*d′* in

http://dx.doi.org/10.5772/55460

oxygenic photosynthesis. BChl *g*/*g*′ may be a convincing ancestor of Chl *a*/*a*′, because the BChl *g*/*g*′ → Chl *a*/*a*′ conversion takes place spontaneously under mild conditions *in vitro* (Kobayashi et al. 1998). Further, a Chl *a*/*a*′ → Chl *d*/*d*′ conversion also occurs with ease *in vitro* (Kobayashi et al. 2005: Koizumi et al. 2005), supporting the succession from the Chl *a*-type cyanobacteria to *A. marina* (Fig. 3). Chl *f* is produced in very small amounts in a Chl *a*-type special cyanobacterium, only when cultivated under NIR light, suggesting that Chl *f* appeared after the birth of Chl *a*. As mentioned above, the primary electron acceptors, $A_0$, are Chl *a*-derivatives even in anoxygenic PS I-type RCs. The secondary electron acceptors are naphthoquinones, and the side chains appear to have been modified after the birth of cyanobacteria, leading to succession from menaquinone to phylloquinone in PS I of oxygenic photosynthetic species (Ohashi et al. 2010).

In Fig. 4, BChl *g*/*g*′ and their derivatives functioning in natural photosynthesis are illustrated. Chlorophyll *a*/*a*′ are produced from BChl *g*/*g*′ by isomerization, and Chl *d*/*d*′ are then produced from Chl *a*/*a*′ by oxidation. These three primed chlorophylls function as the primary electron donors of PS I-type RCs. Note that Chls *b*′ and *f* ′ are not found in natural photosynthesis. Chlorophylls *b* and *f* are produced from Chl *a* by oxidation, but function as antenna pigments.

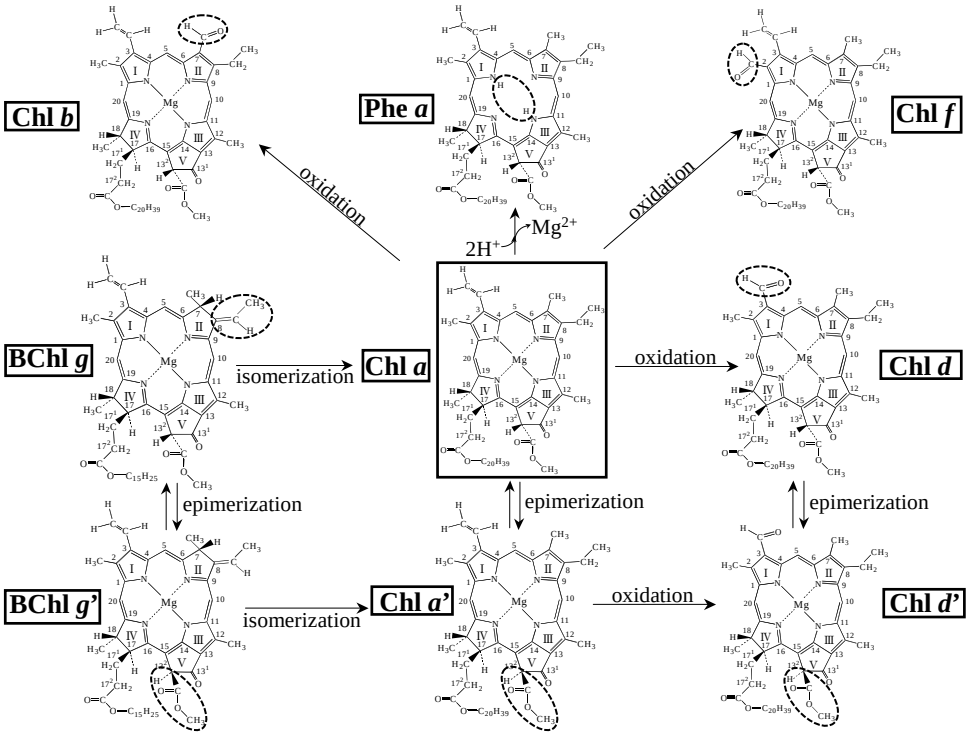


**Figure 4.** Bacterlochlorophyll *g*/*g*′ and their derivatives functioning in natural photosynthesis.

*2.3.2. Pheophytin a as the primary electron acceptor in PS II*

In 1974, pheophytin (Phe) *a* (Fig. 1), a demetallated Chl *a*, was first postulated to be the primary electron acceptor in PS II (Fig. 2) (van Gorkom 1974), and the idea was experimentally confirmed in 1977 (Klimov et al. 1977b). In 1975, bacteriopheophytin (BPhe) *a* was found to function as a primary electron acceptor in the RC of purple bacteria (Fig. 2) (Parson et al. 1975; Rockley et al. 1975; Fajer et al. 1975; Kaufmann et al. 1975), and shortly thereafter BPhe *b* was also found to perform the same function (Fig. 2) (Klimov et al. 1977c). In 1986, BPhe *a* was also found to function in green filamentous bacteria (Fig. 2) (Kirmaier et al. 1986; Shuvalov et al. 1986). In 2001, the primary electron acceptor of PS II in *A. marina* was first found to be Phe *a* (Fig. 2) (Akiyama et al. 2001) and later supported by Tomo et al. (2007). For more details, see Chapter 4 in Kobayashi et al. (2006) and a review by Ohashi et al. (2008).

It is of interest to note that Phe *a* as well as Chl *a'*, *d'* and Chl *d* are artifacts easily produced *in vitro* (see Fig. 4): Phe *a* can be readily produced from Chl *a* under acidic conditions, primed chlorophylls from non-primed ones by epimerization under basic conditions, and Chl *d* from Chl *a* under oxidative conditions. These artifacts, however, function as key components in natural photosynthesis, while Phes *b*, *d*, *f* and Chls *b'*, *f'* are not found in nature.

## 3. Physicochemical properties of chlorophylls *in vitro*

### 3.1. HPLC

In the late 1970s, the high performance liquid chromatography (HPLC) technique was applied to the separation of plant pigments. In many cases the reversed-phase HPLC was preferred (Eskins et al. 1977; Shoaf et al. 1978; Schoch et al. 1978), and is still the main option to date. In that system, however, an eluent gradient is usually required for simultaneous separation of Chls and Phes and the gradient system is unfavorable for quantitative analysis, since the molar absorptivities of pigments strongly depend on solvents. In this context, an isocratic eluent system is favorable. In 1978, a simultaneous separation of Chls and Phes by normal-phase HPLC was attained by an isocratic procedure (Iriyama et al. 1978). In 1984, the isocratic normal-phase HPLC was established as a powerful tool for chlorophyll analysis (Watanabe et al. 1984).

*3.1.1. Mixture of chlorophylls and pheophytins*

Chls *a* and *b* were extracted with acetone/methanol (7/3, *v*/*v*) mixure at 277 K from parsley (*Petroselinum crispum* Nym.), Chl *d* from *A. marina*, and Chl *f* from a cyanobacterium strain KC1 grown under near-infrared LED light. The extract was applied to a preparative-scale HPLC (Senshupak 5251-N, 250 mm x 20 mm i.d.) and eluted with hexane/2-propanol/methanol (100/2/0.4, *v*/*v*) at a flow rate of 7 mL $min^{-1}$ at 277 K, as described elsewhere (Kobayashi et al. 1991). Other authentic pigments, Chl *a'*, Chl *f'*, Phe *a* and Phe *f*, were prepared by epimerization and pheophytinization of Chl *a* and Chl *f* as described elsewhere (Watanabe et al. 1984).

http://dx.doi.org/10.5772/55460

A mixture of Chls and Phes was injected into a silica HPLC column (YMC-pak SIL, 250 x 4.6 mm i.d.) cooled to 277 K in an ice-water bath. The pigments were eluted isocratically with degassed hexane/2-propanol/methanol (100/0.7/0.2, *v/v*) at a flow rate of 0.9 mL $min^{-1}$, and were monitored with a JASCO UV-970 detector ($\lambda$ = 670 nm) and a JASCO Multiwavelength MD-915 detector ($\lambda$ = 300 - 800 nm) in series.

As illustrated in Fig. 6(F), eight Chls and four Phes are clearly separated. One can easily see that *Synechocystis* sp. PCC6803 possesses Phe *a* and Chl *a'* as well as Chl *a*, and that *Chlorella vulgaris* has also Chl *b*.

*3.1.2. Pigment extract from A. marina*

Pigments were extracted from cell suspension (ca. 10 μL) by sonication in a ca. 300-fold volume of acetone/methanol (7/3, *v/v*) mixture for 2 min in the dark at room temperature. The extract was filtered and dried *in vacuo*. The whole procedure was completed within 5 min. The solid material thus obtained was immediately dissolved in 10 μL of chloroform, and injected into a silica HPLC column.

As seen in Fig. 6(C), *A. marina* has three minor chlorophylls, Phe *a*, Chl *a* and Chl *d'*, in addition to the major Chl *d* (Akiyama et al. 2001). Pheophytin *a* functions as the primary electron acceptor in PS II, Chl *a* as the primary electron acceptor in PS I, and Chl *d'* as the primary electron donor P740 as a heterodimer of Chl *d*/*d'*, like the Chl *a*/*a'* in P700 (Fig. 2).

*3.1.3. Pigment extract from strain KC 1*

Cells of the cyanobacterium strain KC1 were grown in BG-11 medium in a glass cell culture flask (1 L) at 297 K with continuous air-bubbling. Cells were incubated under continuous white fluorescent light (50 μmol photons/$m^2$/s) or near-infrared LED light (see Fig. 5A, Tokyorika, Tokyo). Cells at the early stationary phase were harvested by centrifugation. See Akutsu et al. (2011) for more details.

Typical HPLC traces for acetone/methanol extracts from cells of the cyanobacterium strain KC1 cultivated under white fluorescent light or NIR LED light are shown in Figs. 6D and E, respectively. A large amount of Chl *a*, as well as small amounts of Chl *a'* and Phe *a*, were detected in both cells. We should note that only the strain KC1 grown under NIR LED light showed the presence of Chl *f* as a minor pigment and that Chl *f'* and Phe *f* were not detected at all (Fig. 6E).

**3.2. Absorption spectra in four solvent varieties**

The absorption spectrum is the simplest, most useful and extensively used analytical property to characterize chlorophylls. Absorption spectra of Chls show the electronic transitions along the x axis of the Chl running through the two nitrogen (N) atoms of rings II and IV, and along the y-axis through the N atoms of rings I and III (see Fig. 1). The two main absorption bands in the blue and red regions are called Soret and Q bands, respectively, and arise from $\pi \rightarrow \pi^*$ transitions of four frontier orbitals (Weiss 1978; Petke et al. 1979; Hanson 1991).

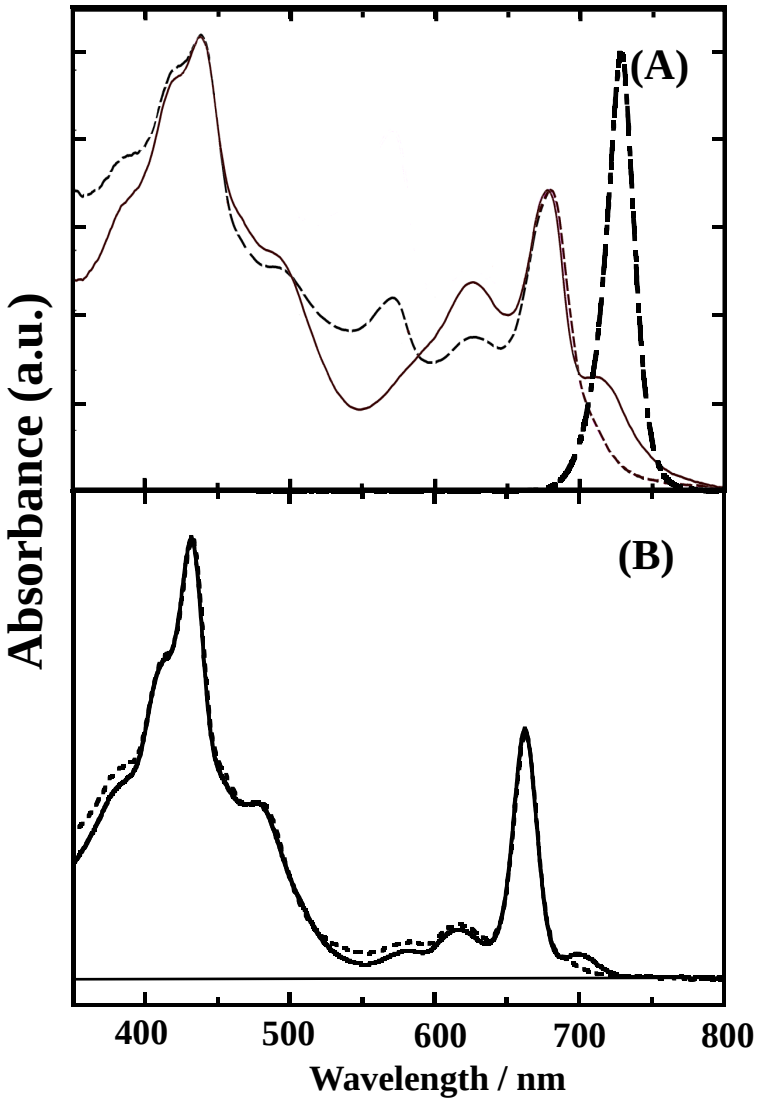


**Figure 5.** Absorption spectra of (A) the cells of strain KC1 grown under white fluorescent light (- - -), near infrared (NIR) LED light (—) and (B) acetone solution of acetone/methanol extracts from the corresponding KC1 cells. Emission spectrum of NIR LED (-•-•-) is inserted in (A).

http://dx.doi.org/10.5772/55460

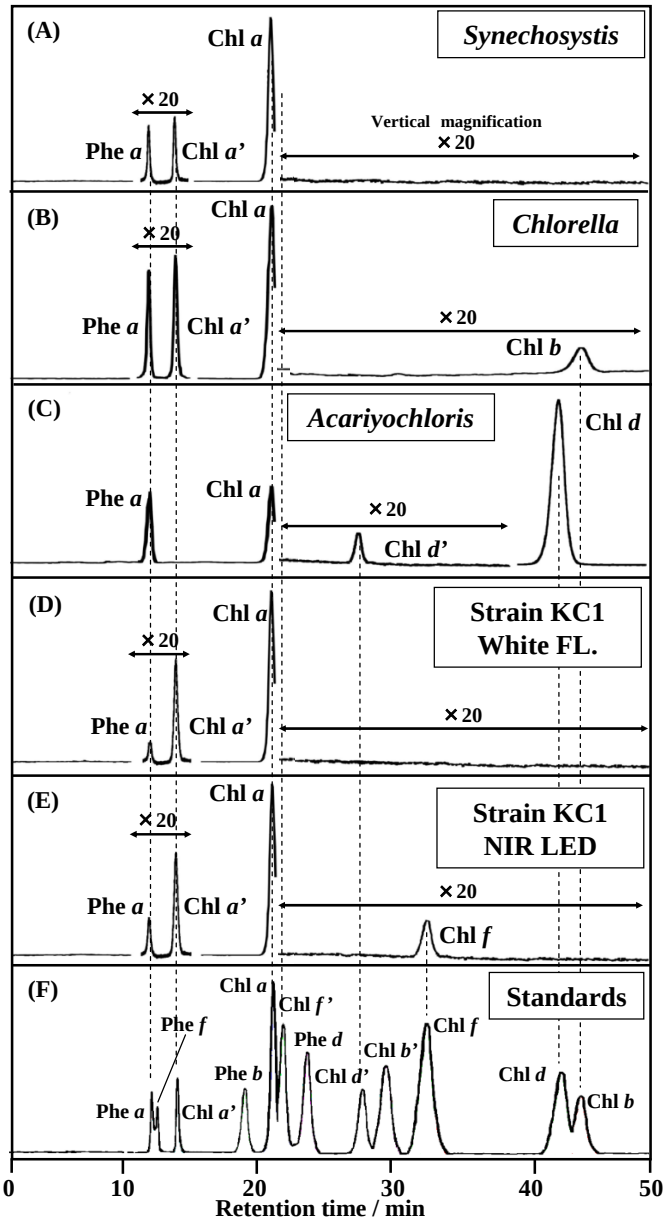


**Figure 6.** Normal-phase HPLC profiles for acetone/methanol extracts of (A) *Synechocystis* sp. PCC6803, (B) *Chlorella vulgaris*, (C) *A. marina*, (D) the cyanobacterium strain KC1 grown under white fluorescent light, (E) the cyanobacterium strain KC1 grown under near-infrared LED light, and (F) a mixture of Chls and Phes. Detection wavelength is 670 nm.

### *3.2.1. Chlorophylls a, b, d and f*

Absorption spectra of Chls *a*, *b*, *d* and *f* in four kinds of solvent measured at room temperature are shown in Fig. 7 (top). As compared to Chl *a*, Chl *b* shows red-shifted Soret bands and blue-shifted weak $Q_Y$ bands, while the $Q_Y$ bands of Chls *d* and *f* are intensified and shifted to longer wavelengths. The Qx exhibits practically no intensity. The ratios of Soret/$Q_Y$ band intensities show remarkable differences, *e.g.*, in diethyl ether ca. 1.3 in Chl *a*, ca. 2.8 in Chl *b*, ca. 0.85 in Chl *d*, and ca. 0.65 in Chl *f* (Table 1). Note that the Soret/$Q_Y$-band ratios in Chl *b* is more than 2 and those in Chls *d* and *f* are below 1 in all solvents in Fig. 7, while the ratios of Chl *a* in three solvents excluding methanol are around 1.3, but slightly below 1 in methanol. So one can easily distinguish Chl *b* from Chls *a*, *d* and *f*; also Chl *a* from Chls *d* and *f*, by their absorption spectra in any solvents used here.

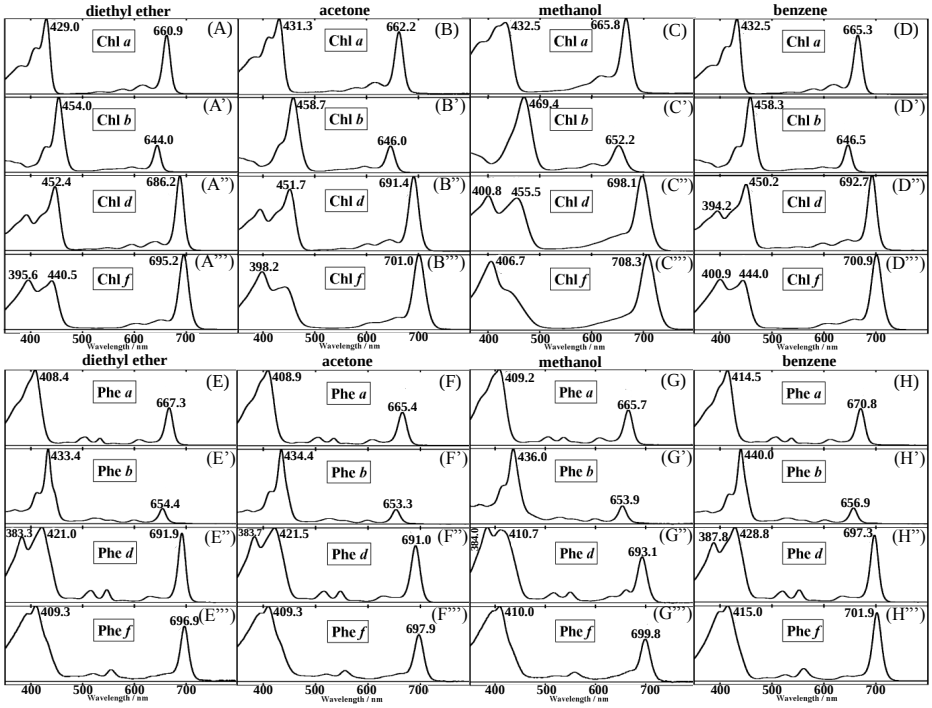


**Figure 7.** Comparison of the absorption spectra of Chls *a*, *b*, *d*, *f* (top), and Phes *a*, *b*, *d*, *f* (bottom) in diethyl ether, acetone, methanol and benzene at room temperature. Spectra were scaled to the Soret- or $Q_Y$-band maximum.

http://dx.doi.org/10.5772/55460

| Compound | $\lambda_{max,blue}$ [nm] | $\lambda_{max,red}$ [nm] | |
|---|---|---|---|
| | (ε[$10^3$ $M^{-1}cm^{-1}$]) | (ε[$10^3$ $M^{-1}cm^{-1}$]) | Ref |
| Chl *a* | 428.4 | 660.3 | Watanabe *et al.* (1984) |
| | (115) | (89.8) | ibid. |
| | 429.1[b] | 661.6[b] | ibid. |
| | (100)[b] | (81.3)[b] | ibid. |
| | 432.5[d] | 665.4[d] | ibid. |
| | (101)[d] | (79.7)[d] | ibid. |
| | 429.0 | 660.9 | Kobayashi *et al.*(2006) |
| | (1.00)[a] | (0.775)[a] | ibid. |
| | 431.3[b] | 662.2[b] | This work |
| | (1.00)[a,b] | (0.828)[a,b] | ibid. |
| | 432.5[c] | 665.8[c] | ibid. |
| | (0.944)[a,c] | (1.00)[a,c] | ibid. |
| | 432.5[d] | 665.3[d] | ibid. |
| | (1.00)[a,d] | (0.785)[a,d] | ibid. |
| Phe *a* | 408.4 | 667.9 | Watanabe *et al.* (1984) |
| | (107) | (52.6) | ibid. |
| | 409.2[b] | 665.9[b] | ibid. |
| | (104)[b] | (46.0)[b] | ibid. |
| | 414.8[d] | 671.6[d] | ibid. |
| | (108)[d] | (53.1)[d] | ibid. |
| | 408.4 | 667.3 | Kobayashi *et al.*(2006) |
| | (1.00)[a] | (0.497)[a] | ibid. |
| | 408.9[b] | 665.4[b] | This work |
| | (1.00)[a,b] | (0.440)[a,b] | ibid. |
| | 409.2[c] | 665.7[c] | ibid. |
| | (1.00)[a,c] | (0.464)[a,c] | ibid. |
| | 414.5[d] | 670.8[d] | ibid. |
| | (1.00)[a,d] | (0.798)[a,d] | ibid. |
| Chl *b* | 451.9 | 641.9 | Watanabe *et al.* (1984) |
| | (159) | (56.7) | ibid. |
| | 455.8[b] | 644.6[b] | ibid. |
| | (136)[b] | (47.6)[b] | ibid. |

| Compound | $\lambda_{max,blue}$ [nm] ($\varepsilon[10^3\ M^{-1}cm^{-1}]$) | $\lambda_{max,red}$ [nm] ($\varepsilon[10^3\ M^{-1}cm^{-1}]$) | Ref |
|---|---|---|---|
| | 457.9[d] | 646.2[d] | ibid. |
| | (152)[d] | (56.2)[d] | ibid. |
| | 452.4 | 642.5 | Kobayashi *et al*.(2006) |
| | (1.00)[a] | (0.355)[a] | ibid. |
| | 458.7[b] | 646.0[b] | This work |
| | (1.00)[a,b] | (0.355)[a,b] | ibid. |
| | 469.4[c] | 652.2[c] | ibid. |
| | (1.00)[a,c] | (0.355)[a,c] | ibid. |
| | 458.3[d] | 646.5[d] | ibid. |
| | (1.00)[a,d] | (0.364)[a,d] | ibid. |
| Phe *b* | 432.7 | 654.6 | Watanabe *et al.* (1984) |
| | (172) | (34.8) | ibid. |
| | 433.8[b] | 653.3[b] | ibid. |
| | (153)[b] | (29.3)[b] | ibid. |
| | 439.5[d] | 656.7[d] | ibid. |
| | (152)[d] | (4.718)[d] | ibid. |
| | 433.2 | 654.5 | Kobayashi *et al*.(2006) |
| | (1.00)[a] | (0.202)[a] | ibid. |
| | 434.4[b] | 653.3[b] | This work |
| | (1.00)[a,b] | (0.195)[a,b] | ibid. |
| | 436.0[c] | 653.9[c] | ibid. |
| | (1.00)[a,c] | (0.245)[a,c] | ibid. |
| | 440.0[d] | 656.9[d] | ibid. |
| | (1.00)[a,d] | (0.216)[a,d] | ibid. |
| Chl *d* | 447 | 688 | Smith and Benitez (1955) |
| | (87.6) | (98.9) | ibid. |
| | 447 | 688 | French (1960) |
| | (87.6) | (98.5) | ibid. |
| | 390, 445 | 686 | Miyashita *et al.* (1997) |
| | 392[b], 447[b] | 688[b] | ibid. |
| | 400[c], 455[c] | 697[c] | ibid. |
| | 445.6 | 686.2 | Kobayashi *et al.*(2006) |

http://dx.doi.org/10.5772/55460

| Compound | $\lambda_{max,blue}$ [nm] | $\lambda_{max,red}$ [nm] | |
|---|---|---|---|
| | (ε[$10^3$ $M^{-1}cm^{-1}$]) | (ε[$10^3$ $M^{-1}cm^{-1}$]) | Ref |
| | (0.853)[a] | (1.00)[a] | ibid. |
| | 394.3[b], 451.7[b] | 691.4[b] | This work |
| | (0.559)[a,b](0.826)[a,b] | (1.00)[a,b] | ibid. |
| | 400.8[c], 455.5[c] | 698.1[c] | ibid. |
| | (0.735)[a,c](0.706)[a,c] | (1.00)[a,c] | ibid. |
| | 394.2[d], 450.2[d] | 693.7[d] | ibid. |
| | (0.532)[a,d], (0.885)[a,d] | (1.00)[a,d] | ibid. |
| Phe *d* | 421 | 692 | Smith and Benitez (1955) |
| | (84.9) | (72.2) | ibid. |
| | 421 | 692 | French (1960) |
| | (84.9) | (72.2) | ibid. |
| | 382.7, 421.3 | 692.0 | Kobayashi *et al*.(2006) |
| | (0.881)[a],(1.00)[a] | (0.911)[a] | ibid. |
| | 383.7[b], 421.5[b] | 691.0[b] | This work |
| | (0.888)[a,b], (1.00)[a,b] | (0.761)[a,b] | ibid. |
| | 384.0[c], 410.7[c] | 693.1[c] | ibid. |
| | (1.00)[a,c], (0.964)[a,c] | (0.637)[a,c] | ibid. |
| | 387.8[d], 428.8[d] | 697.3[d] | ibid. |
| | (0.802)[a,d], (1.00)[a,d] | (0.915)[a,d] | ibid. |
| Chl *f* | 395.6, 440.5 | 695.2 | This work |
| | (0.657)[a] (0.648)[a] | (1.00)[a] | ibid. |
| | 398.2[b], 442.0[b] | 701.0[b] | ibid. |
| | (0.780)[a,c], (0.576)[a,b] | (1.00)[a,b] | ibid. |
| | 400.9[d], 444.0[d] | 700.9[d] | ibid. |
| | (0.668)[a,d], (0.658)[a,d] | (1.00)[a,d] | ibid. |
| | 406.7[c] | 708.3[c] | Akutsu *et al.* (2011) |
| | (0.904)[a,c] | (1.00)[a,c] | ibid. |
| | 406 | 706 | Chen *et al.* (2010) |
| | (1.00)[a,d] | (0.527)[a,d] | ibid. |
| Phe *f* | 409.3 | 696.9 | This work |
| | (1.00)[a] | (0.727)[a] | ibid. |
| | 409.3[b] | 697.9[b] | ibid. |

| Compound | $\lambda_{max,blue}$ [nm] | $\lambda_{max,red}$ [nm] | |
|---|---|---|---|
| | ($\varepsilon$[$10^3$ $M^{-1}cm^{-1}$]) | ($\varepsilon$[$10^3$ $M^{-1}cm^{-1}$]) | Ref |
| | (1.00)[a,b] | (0.610)[a,b] | ibid. |
| | 410.0[c] | 699.8[c] | ibid. |
| | (1.00)[a,c] | (0.561)[a,c] | ibid. |
| | 415.0[d] | 701.9[d] | ibid. |
| | (1.00)[a,d] | (0.776)[a,d] | ibid. |

a: relative values

b: in acetone

c: in methanol

d: in benzene

**Table 1.** Absorption properties of chlorophylls in diethylether at room temperature

It is somewhat difficult to distinguish Chl *f* from Chl *d*, when one roughly compares the absorption spectrum of Chl *f* in diethyl ether (Fig. 7A"') with that of Chl *d* in methanol (Fig. 7C"), because their spectral shapes are very similar. In contrast, in diethyl ether one can easily distinguish Chl *f* from Chl *d* without spectrophotometer, because Chl *f* looks blue-green as Chl *a*, while Chl *d* light-green as Chl *b*, indicating that the naked eye is often powerful for colour judgement.

The Soret bands include several intense bands. In diethyl ether and benzene, the Soret band of Chl *f* is clearly split into two bands, most probably the so-called B-bands (longer wavelength) and η-bands (shorter wavelength), while Chl *d* shows such a split not in those solvents but in methanol, and hence one can easily distinguish them by comparing their optical spectra in the same solvents, *e.g.*, diethyl ether (Figs. 7A" and A"').

In Fig. 5 are shown the absorption spectra of the strain KC1 grown under white fluorescent light and NIR LED light. The cells grown under NIR LED light show a clear shoulder over 700 nm, extending up to almost 800 nm (Fig. 5A). Absorption spectra in acetone solution of acetone/methanol extracts from the KC1 cells cultivated under NIR LED also exhibit a longer wavelength peak in the range of about 690 to 720 nm (Fig. 5B), due to the presence of Chl *f*. We had better pay attention that the NIR LED emission spectrum seen in Fig. 5A overlaps the absorption spectrum of the strain KC1 cells grown under white fluorescent light, indicating that the cells without Chl *f* can absorb NIR LED light, where some Chl *a* molecules possessing longer wavelength absorption may act as a trigger for Chl *f* biosynthesis under NIR LED light. If this hypothesis holds, a much longer wavelength LED could not induce Chl *f* biosynthesis. In such a study, one should give a lot of care to the shorter wavelength foot of emission spectrum of NIR LED not to overlap the absorption of cells at all.

http://dx.doi.org/10.5772/55460

We should note that inductive effects on the absorption wavelengths and intensities of $Q_Y$-bands of chlorophylls strongly depend on the nature and position of substituent(s) on the macrocycle, due to the presence of two different electronic transitions polarized in the x and y directions (the axes of transition moments are depicted in Fig.1) (Gouterman 1961, Gouterman et al. 1963; Weiss 1978; Petke et al. 1979; Hanson 1991, Kobayashi et al. 2006b). Replacement of the electron-donating group, $-CH_3$, on ring II of Chl *a* by the electron-withdrawing group, -CHO, yielding Chl *b*, causes the blue-shift and significant intensity reduction of the $Q_Y$-band (Fig. 7). In contrast, replacement of $-CH_3$ on ring I of Chl *a* by -CHO, yielding Chl *f*, causes the red-shift and intensity increase of the $Q_Y$-band (Fig. 7). A similar phenomenon is clearly seen in Chl *d*, where $-CH=CH_2$ on ring I of Chl *a* is replaced with -CHO. These results indicate it is a general feature that substitution by the electron-withdrawing group on ring II causes the blue-shift and intensity reduction of the $Q_Y$-band and that the same substitution on ring I leads the opposite, namely, the red-shift and intensity increase of the $Q_Y$-band. Moreover, it looks that substitution on ring I by the electron-withdrawing group generates the well-split Soret band, while showing heavy dependence on solvent as described above.

### *3.2.2. Pheophytins a, b, d and f*

The free base related to Chl is called Phe. First of all, we emphasize that in natural photosynthesis only Phe *a* functions, and Phes *b*, *d* and *f* are not functional. In general, the more structured shape and red shifted Soret band of Chls distinguishes them from the corresponding Phes. In contrast to Chls, the η bands in the Soret band was poorly resolved in any Phes except Phe *d* (Fig. 7). Removal of the central Mg increases deviation from planarity and reduces the molecular symmetry, thus increasing Soret and $Q_X$ transition. The Soret/$Q_Y$-band ratios noticeably increases by pheophytinization; in diethyl ether Phe *b* shows the highest value of around 5, Phe *a* the secondary highest about 2, and Phe *d* the lowest near 1 (compare bottom with top in Fig. 7, see also Table 1). Therefore, contamination of pheophytins in a Chl sample is often noticed from the optical spectra.

As seen in Fig. 7, Phe *b* can be easily distinguished from Phe *a* by its blue shifted $Q_Y$-band, red shifted Soret band, and by the marginally higher Soret/$Q_Y$ band ratio. Phes *d* and *f* can be distinguished from Phes *a* and *b* by their red shifted $Q_Y$ band and intense $Q_Y$ bands, i.e., the Soret/$Q_Y$-band ratios in Phes *d* and *f* are not high and almost the same as those seen in Chl *a*. We should also pay attention to Phe *f*, because in methanol its optical shape is somewhat similar to Phe *a* (compare Figs. 7G with 7G'''), although they can be distinguished by the $Q_Y$ wavelength difference. We must emphasize again that Phes possess relatively strong and characteristic $Q_X$-bands in the region of 490-570 nm; the $Q_X$ bands in Phes *a* and *d* are better resolved to the $Q_X(0,0)$ and $Q_X(1,0)$ transitions. Phe *d* also shows significant splitting of the Soret and $Q_X$ bands in all solvents as illustrated in Fig. 7. In contrast, the $Q_x$ band corresponding to the $Q_X(1,0)$ transition (shorter wavelength) of Phe *f* looks unclear. It is of interest to note that in diethyl ether Phe *d* assumes a pale pink color, while both Phes *b* and *f* show a dull color. These characteristics will help us to discern Phes from Chls, and among Phes.

### 3.3. Circular dichroism spectra

Circular dichroism (CD) spectra are very useful for distinction between the primed chlorophyll, *e.g.*, Chl *a'*, and the corresponding non-primed one, Chl *a*, although the absorption characteristics of the primed derivatives (Chls *a'*, *b'*, *d'*, *f'*, Phes *a'*, *b'*, *d'* and *f'*) are identical with those of the non-primed ones (Wolf and Scheer 1973; Weiss 1978; Watanabe et al. 1984; Kobayashi et al. 2006b).

A spectropolarimeter Model FDCD-309 (JASCO) was used for CD measurements. Benzene was chosen as the solvent, in view of the sufficiently slow interconversion between epimeric species in this medium (Watanabe et al. 1984). The spectra were recorded from 800 nm to 300 nm at a scan rate of 200 nm/min with 20 scans at room temperature; time for measurement was ca. one hour.

The CD spectra of Chl *a*/*a'*, *b*/*b'*, *d*/*d'* and *f*/*f'* in benzene are illustrated in Fig. 8. It is immediately seen that, for a given pair of epimers, the CD spectra are considerably different, although the absorption spectra are practically identical with each other. For each of Chls *a'*, *b'*, *d'* and *f'*, an intense negative CD is associated with $Q_Y(0,0)$ and a well-defined weakly negative satellite with $Q_Y(1,0)$. On the other hand, the non-primed species, Chls *a*, *b*, *d* and *f*, show complicated, very weak negative and/or positive activities at these transitions. In Fig. 9, all pheophytins show negative activities, and primed ones reveal stronger and red-shifted signals compared to the non-primed ones, although the absorption spectra of the primed derivatives are also identical with those of the non-primed ones. The findings suggest that the $Q_Y$ maximum transition consists of at least two bands, and shorter wavelength band shows stronger activity in primed Phe and longer wavelength band stronger in non-primed Phe.

A series of $Q_X$ transitions occur in the "valley" of the absorption spectrum as described in section 2. The positive CD activities derived from the $Q_X(0,0)$ absorption (called bands III, see Fig. 2 in Petke et al. 1979) appear at 579, 535, 594, 557, 548, 604, 567 and 559 nm for Chl *a'*, Phe *a'*, Chl *d'*, Phes *d*, *d'*, Chl *f'*, Phes *f* and *f'*, respectively, while Chl *f* and Phe *a* exhibit weakly negative activities at 609 nm and 535 nm, respectively. Such definite activities are not observed in Chls *a*, *b*/*b'*, *d* and Phe *b*/*b'*; optical activities of *b*-type pigments, Chl *b*/*b'* and Phe *b*/*b'*, are extremely weak, which may be related to the very diffuse feature of their absorption spectra. The CD activity associated with the $Q_X(0,1)$ absorption satellites (band IV) at the shorter wavelength also is very weak and vague in all the pigments examined.

The Chl and Phe Sorets contain many $\pi$-$\pi^*$ transitions characterized by a complex mixture of configurations. According to the results of molecular orbital calculations (Weiss 1978; Petke et al. 1979; Hanson 1991), band B in the Soret absorption consists of two nearly degenerate electronic transitions, $B_X(0,0)$ and $B_Y(0,0)$. All the primed derivatives gave single and strongly positive CD spectra at this absorption peak, suggesting that the two transitions contribute to CD spectra in a similar manner (Watanabe et al. 1984). In contrast, the CD spectra of non-primed species, except Chl *f* and Phes, apparently reflect the existence of the two transitions: they show a maximum and a minimum with the center wavelength roughly coinciding with the Soret absorption maximum. Different feature of CD spectrum for Chl *f* among Chls may come from its characteristically splitted Soret absorption arising from B-bands and so-called

http://dx.doi.org/10.5772/55460

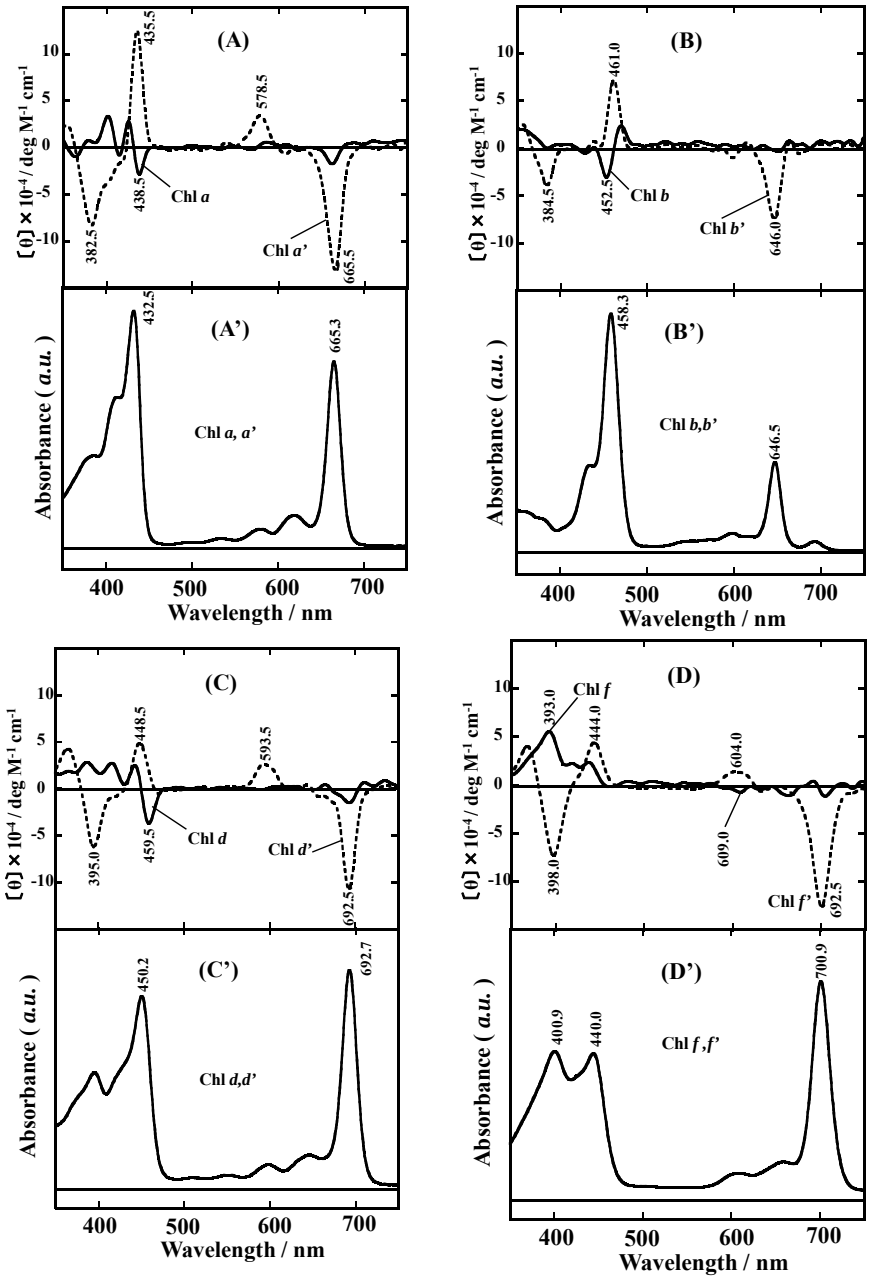


**Figure 8.** CD spectra for (A) Chls *a*/*a'*, (B) Chls *b*/*b'*, (C) Chls *d*/*d'*, (D) Chls *f*/*f'*, and (A')-(D') the corresponding absorption spectra in benzene at room temperature. [*θ*] denotes the molar ellipticity.

η-bands in benzene. Primed Chls exhibit relatively intense negative CD spectra in the near ultraviolet at η-bands of the Soret region (Welss 1978; Petke et al. 1979), whereas non-primed ones exhibit positive activities. Phes *a* and *f* also show positive CD spectra at η-bands in the near ultraviolet region, but such a tendency is not clear in Phe *b*, and Phe *d* exhibits negative activity (Fig. 9), although all the primed Phes show negative activity and Phe *d'* shows the most intense activity.

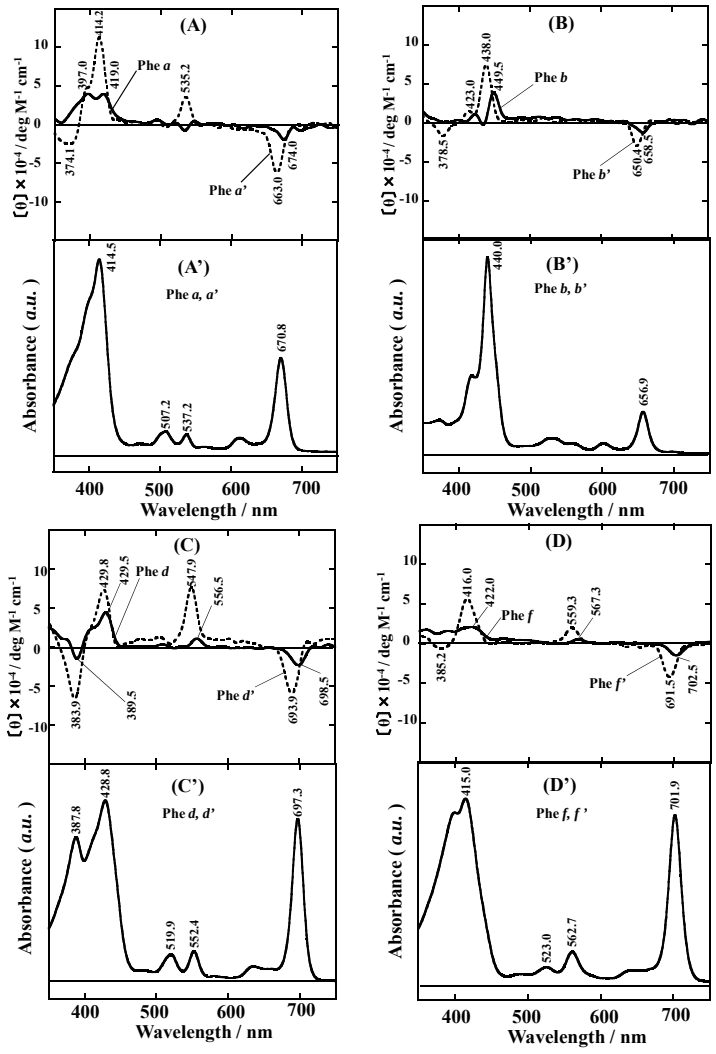


**Figure 9.** CD spectra for (A) Phes *a*/*a'*, (B) Phes *b*/*b'*, (C) Phes *d*/*d'*, (D) Phes *f*/*f'*, and (A')-(D') the corresponding absorption spectra in benzene at room temperature. [*θ*] denotes the molar ellipticity.

http://dx.doi.org/10.5772/55460

### 3.4. Mass spectra

Chlorophylls in natural photosynthesis are sometimes present in very small amounts, and hence the use of mass spectrometry (MS) can be advantageous since only minute samples are required. MS can provide accurate and useful information not only on molecular weights and elemental compositions but also on the nature of functional groups attached to the macrocycle (*e.g.* phytol) and of the central metal (see reviews by Smith 1975; Hunt and Michalski 1991; Porra and Scheer 2000; Kobayashi et al. 2006).

LC/MS experiments were performed on an LCQ mass spectrometer (Thermo Fisher Scientific Inc., MA, U.S.A.) equipped with an HPLC system (HP1100, Agilent, CA, U.S.A.) connected with a diode array detector. Each sample dissolved in dichloromethane before analysis was applied on a JASCO Finepak SIL C18S column (150 mm x 4.6 mm i.d.) cooled to 277 K in an ice-water bath, and separated using a mixture of ethanol/methanol/2-propanol/water (86/13/1/3, *v*/*v*) at a flow rate of 300 μL $min^{-1}$. The eluate was monitored by the UV-Vis absorption in a range of 220-800 nm, and was introduced into the mass spectrometer from 5 to 55 min after sample injection. Atmospheric pressure chemical ionization (APCI) mass and MS/MS spectra were recorded in the positive-ion mode in the mass range of *m*/*z* 150-2,000. Helium was used as collision gas for MS/MS experiments, followed by the isolation of ions over a selected mass window of 2 Da. The mass spectrometer was initially tuned using a standard Chl *a* solution as follows: APCI vaporizer temp., 723 K; spray voltage, 4 kV; capillary temperature, 423 K; capillary voltage, 8 V; sheath gas (nitrogen); flow rate, 56 (arbitrary unit); auxiliary gas flow rate, 9 (arbitrary unit).

As illustrated in Fig. 10 (left), Chl *a* ($C_{55}H_{72}MgN_4O_5$, monoisotopic mass; 892.535. Hereafter the value in the bracket shows the monoisotopic mass of the molecule or the ion) gives the protonated molecule ($[M+H]^+$) at *m*/*z* 893.2 producing the dominant fragment ion at *m*/*z* 615.1. The mass difference 278 between $[M+H]^+$ and the product ion corresponds to $C_{20}H_{38}$. This shows the presence of a phytyl chain in Chl *a*. The other product ions at *m*/*z* 583.0 and *m*/*z* 555.2 corresponding to $[M+H-278-32]^+$ and $[M+H-278-60]^+$, respectively, are supposed to be the results of the loss of carboxymethyl group followed by the cleavage of phytol. The losses of 278, 310 and 338 from the precursor ion in MS/MS spectra are seen in all the pigments examined here reveals the presence of a phytyl chain.

It is interesting to note that a typical fast atom bombardment (FAB)-mass spectrum of Chl *a* shows two intense molecular ion peaks, $[M]^+$ at *m*/*z* 892.6 and $[M + H]^+$ at 893.6, as well as the dominant fragment ion $[M-C_{20}H_{38}+H]^+$ at *m*/*z* 614.3 (see Fig. 4 in Kobayashi et al. 2000). Both spectra, however, reveal that Chl *a* has a phytyl chain ($C_{20}H_{39}$). We should make sure that the mass spectra of chlorophyll molecular ion peak(s) and the fragment ion peak(s) vary by *m*/*z* 1.0 according to the ionization methods.

Chlorophyll *d* ($C_{54}H_{70}MgN_4O_6$, 894.515) gives the protonated molecule ($[M+H]^+$) at *m*/*z* 895.2 and the prominent fragment ion at *m*/*z* 617.1. Though chlorophylls *b* and *f* (both $C_{55}H_{70}MgN_4O_6$, 906.515) are eluted at different LC retention times, they show the same mass and MS/MS spectral patterns, $[M+H]^+$ at *m*/*z* 907 and the dominant product ion at *m*/*z* 629, which correspond to $[C_{55}H_{71}MgN_4O_6]^+$ (907.522) and $[M-C_{20}H_{38}+H]^+$ (629.225). These results

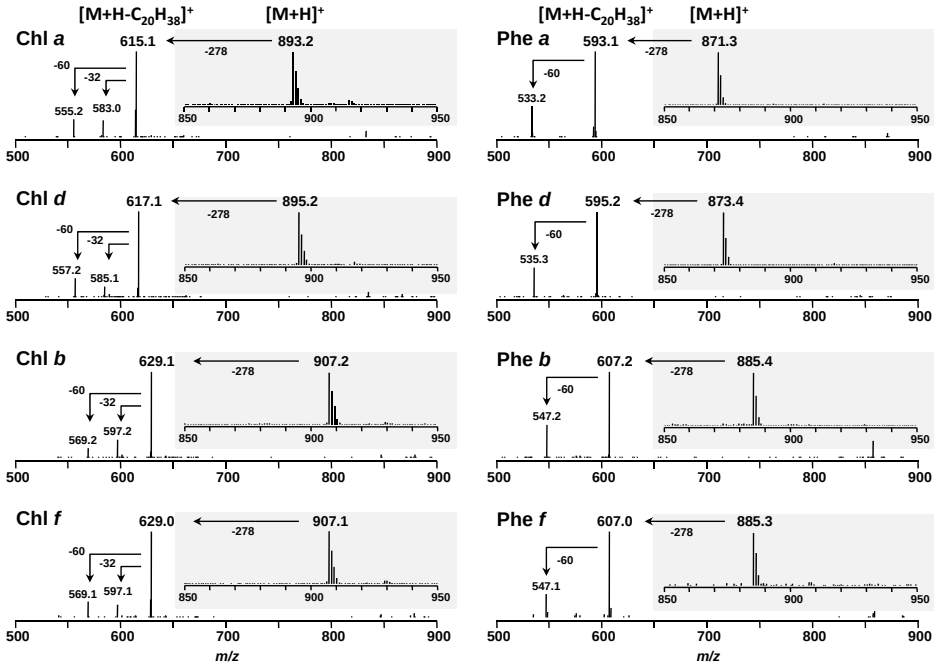


**Figure 10.** MS/MS spectra of Chls *a*, *b*, *d*, *f* (left column) and Phes *a*, *b*, *d* and *f* (right column). Each mass spectrum of the chlorophyll fraction is shown in the shaded square. MS/MS spectra of the protonated molecules ($[M+H]^+$) of Chls *a*, *b*, *d* and *f* give product ions of $[M+H-278]^+$, $[M+H-278-32]^+$ and $[M+H-278-60]^+$. Pheophytins *a*, *b*, *d* and *f* give product ions of $[M+H-278]^+$ and $[M+H-278-60]^+$.

suugest that Chl *f* also possesses a phythyl long chain in such molecules as Chls *a*, *b* and *d*, and that most probably one -$CH_3$ moiety of Chl *a* is substituted for -CHO group in Chl *f* like Chl *b*, yielding [2-formyl]-Chl *a*, [12-formyl]-Chl *a* or [18-formyl]-Chl *a*.

As seen in Fig. 10 (right), the corresponding pheophytins prepared by acid treatment clearly showed the absence of magnesium (Fig. 1). For example, $[M+H]^+$ of Phe *a* is observed at *m/z* 871.3 which is 22 Da smaller than that of Chl *a*, showing the substitution of Mg with two H atoms by pheophytinization (see Fig. 1). Pheophytins *b* and *f* ($C_{55}H_{74}N_4O_6$, 884.545) and Phe *d* ($C_{54}H_{72}N_4O_6$ 872.545) show the similar pattern, supporting that all of them do not possess Mg as central metal.

### 3.5. Nuclear magnetic resonance spectra

Nuclear magnetic resonance (NMR) spectroscopy can offer ample information about the molecular structure. Coupled use of NMR with HPLC, absorption-, CD- and mass-spectrometries has not only definitively identified the structures of several major naturally-occurring Chls but has also assisted recent studies of minor Chl pigments, present in minute quantities, such as electron donors and acceptors in the RC.

http://dx.doi.org/10.5772/55460

The NMR spectra were recorded on a Bruker Avance 800 spectrometer (Bruker Biospin, Karlsruhe, Germany), with a frequency of $^{1}$H at 800 MHz and $^{13}$C at 201 MHz, equipped with TCI CryoProbe using a microtube (Shigemi Inc., Tokyo) and about 0.5 mg of sample in 0.3 mL of acetone-$d_6$ with tetramethylsilane (TMS) as an internal standard. The chemical shifts are given in δ-scale [ppm] downfield from TMS. The measurements were performed at 273 K. The typical experimental conditions for the $^{1}$H NMR spectra were 256 scans, a spectral width of 17 ppm, 128k data points. The $^{13}$C spectra were acquired using a power gated decoupling with 48k scans. The spectral width of 220 ppm was acquired in 64k data points. The 2D-homonuclear (Nuclear Overhauser and Exchange Spectroscopy (NOESY)) and 2D-heteronuclear (H,C-Heteronuclear Single Quantum Coherence (H,C-HSQC) and H,C-Heteronuclear Multiple Bond Correlation (H,C-HMBC)) experiments were performed for the structural assignments of the $^{1}$H and $^{13}$C signals using standard 2D-NMR pulse sequences of Bruker software.

### *3.5.1. $^{1}$H-NMR*

As observed in one-dimensional $^{1}$H-NMR spectra (Fig. 11, Table 2), marked differences are seen in the signals arising from the formyl group. Each low-field singlet signal characteristic of the formyl moiety observed around 11 ppm in the spectra of Chls *b* ($7^{1}$), *d* ($3^{1}$) and *f* ($2^{1}$) is absent from the spectrum of Chl *a*. Similarly, double doublet signal of $3^{1}$-H vinylic proton at 8-8.5 ppm in the spectra of Chls *a*, *b* and *f* is not seen in the spectrum of Chl *d*. These results reconfirm that Chl *d* is 3-desvinyl-3-formyl Chl *a* ([3-formyl]-Chl *a*).

Here we note that the $3^{1}$-H vinylic proton shows a large downfield shift in Chl *f* (8.534 ppm) and that is slightly upfield shifted in Chl *b* (8.043 ppm), as compared to Chl *a* (8.162 ppm), suggesting that Chl *f* should be formylated along the y-axis and that interaction between -CH=$CH_2$ and -CHO in Chl *f* is rather strong than that in Chl *b*. The -CHO substitution position in Chl *f* is hence most probably at C2, next to the 3-vinyl group.

The pair signals of $3^{2}$- and $3^{2'}$-H vinylic protons are well resolved in the spectra of Chls *a* (6.242 ppm and 6.028 ppm) and *b* (6.302 ppm and 6.055 ppm), while the corresponding pair signals in Chl *f* show low resolution (6.365 ppm and 6.324 ppm), suggesting that the environment of 3-vinyl moiety in Chls *a* and *d* is very similar to each other, but is profoundly different from that in Chl *f*, most probably due to the presence of formyl moiety at the neighboring C2 in Chl *f*. The $^{1}$H singlet signals for $7^{1}$-$CH_3$ in Chls *a*, *d* and *f* are at 3.3 ppm and absent from the spectrum of Chl *b*, while the $^{1}$H signal for $7^{1}$-CHO in Chl *b* appears on a much lower field at 11.3 ppm. Another marked difference seen in Chl *f* spectrum is the disappearance of the singlet signal of $2^{1}$-$CH_3$ proton; the corresponding signals are observed at 3.3-3.72 ppm in the spectra of Chls *a*, *b* and *d*, implying that $2^{1}$-$CH_3$ of Chl *a* is substituted in Chl *f* for some other moiety, most probably -CHO. No other change is clear in the one-dimensional $^{1}$H-NMR spectra.

### *3.5.2. $^{13}$C-NMR*

In the $^{13}$C-NMR spectra (Fig. 12, Table 3), marked differences are noted in the range of 0 ppm to 20 ppm, 120 ppm to 140 ppm, and 180 ppm to 200 ppm, relating to the -$CH_3$, -CH=$CH_2$ and -CHO moieties. Compared to Chl *a*, in the spectrum of Chl *f*, the $^{13}$C signal of $2^{1}$-$CH_3$ is absent,

the $7^1$-$CH_3$ and $3^1$,2-CH=$CH_3$ carbon signals appear at 11 ppm, 130 ppm and 126 ppm, respectively, similar to Chl *a* (11 ppm, 131 ppm and 120 ppm). Further, a new carbon signal appears at 189 ppm, close to the signals of -CHO in Chls *b* (188 ppm) and *d* (190 ppm), supporting the presence of -CHO at C2 in Chl *f*.

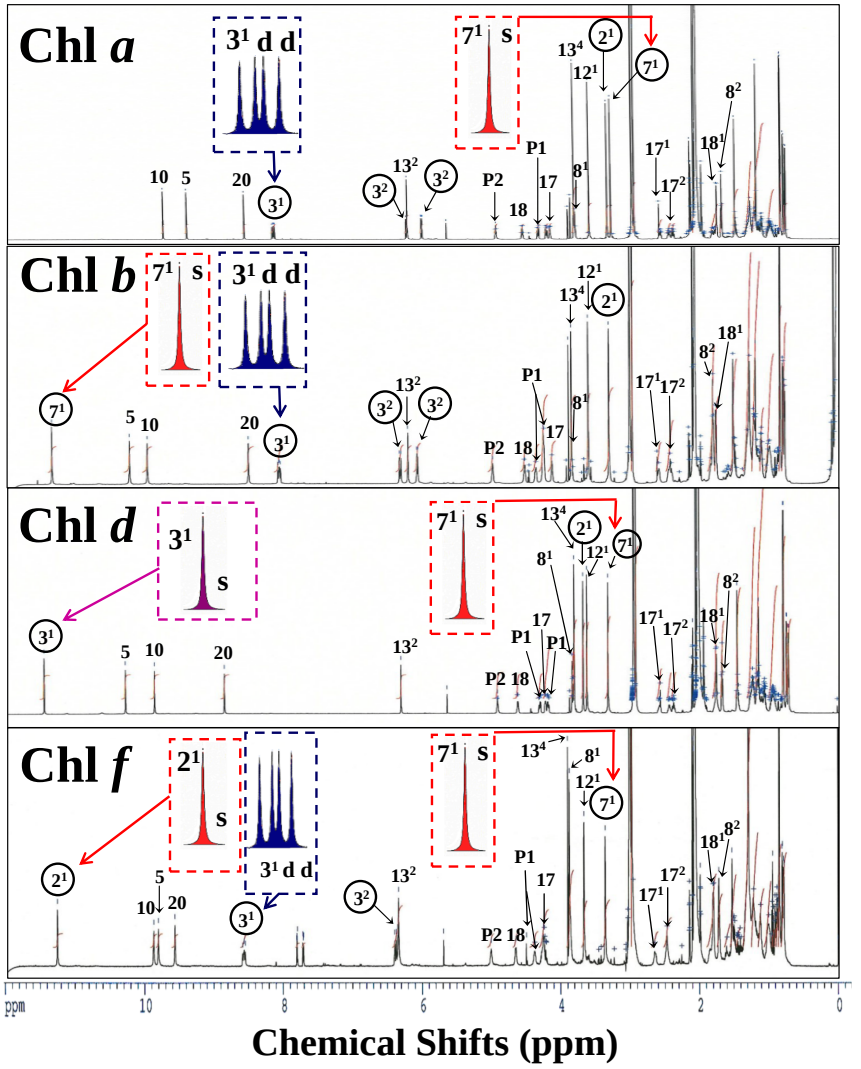


**Figure 11.** $^1$H-NMR spectra of Chls *a*, *b*, *d* and *f* measured in acetone-$d_6$ at 273 K. Signals corresponding to $^1$H atoms of the macrocycle are labeled with the numbers of the corresponding carbons. The peak at 2.06-2.11 ppm is acetone and 3.07-3.10 ppm is $H_2O$, respectively.

http://dx.doi.org/10.5772/55460

| IUPAC no.of carbon atom | Chl a | Chl b | Chl d | Chl f |
|---|---|---|---|---|
| 2[1] | 3.343 (3.36)[1] (s) | 3.316 (3.40)[2*](s) | 3.724 (3.68)[3](s) | 11.215 (11.35)[4**](s) |
| 3 | - | - | - | - |
| 3[1] | 8.162 (8.18)[1](dd) | 8.043(7.95)[2*](dd) | 11.460 (11.40)[3](s) | 8.534(dd) |
| 3[2] | 6.242 (6.24)[1](dd), 6.028 (6.03)[1](dd) | 6.302(6.25)[2*](dd), 6.055 (6.04)[2*](dd) | - | 6.324(dd), 6.365(dd) |
| 4 | - | - | - | - |
| 5 | 9.410 (9.40)[1](s) | 10.192 (10.04)[2*](s) | 10.294(10.20)[3](s) | 9.770 (9.79)[4**](s) |
| 7[1] | 3.300 (3.30)[1](s) | 11.305 (11.22)[2*](s) | 3.365 (3.33)[3](s) | 3.351(s) |
| 8 | - | - | - | - |
| 8[1] | 3.817 (3.82)[1](q) | 4.243 | 3.876 (3.86)[3](q) | 3.754(q) |
| 8[2] | 1.696 (1.69)[1](t) | 1.815 | 1.723 (1.73)[3](t) | 1.705(t) |
| 10 | 9.749 (9.75)[1](s) | 9.934 (9.64)[2*](s) | 9.873 (9.8)[3](s) | 9.838 (9.86)[4**](s) |
| 11 | - | - | - | - |
| 12 | - | - | - | - |
| 12[1] | 3.619 (3.61)[1](s) | 3.606 (3.65)[2*](s) | 3.668 (3.65)[3](s) | 3.637(s) |
| 13 | - | - | - | - |
| 13[2] | 6.234 (6.24)[1](s) | 6.189 (6.19)[2*](s) | 6.335 (6.28)[3](s) | 6.318(s) |
| 13[3] | - | - | - | - |
| 13[4] | 3.829 (3.83)[1](s) | 3.842 (4.02)[2*](s) | 3.851 (3.83)[3](s) | 3.887(s) |
| 17 | 4.175 (4.16)[1] | 4.128 | 4.242 (4.25)[3] | 4.230 |
| 17[1] | 2.589 (2.60)[1], 2.461 (2.45)[1] | 2.43,2.593 | 2.484,2.622 | 2.467,2.632 |
| 17[2] | 2.431 (2.35)[1], 2.159 (2.05)[1] | 2.08,2.44 | 1.98,2.418 | 2.08,2.47 |
| 18 | 4.572 (4.57)[1](q) | 4.524(q) | 4.660 (4.63)[3](q) | 4.634(q) |
| 18[1] | 1.772 (1.77)[1], 1.762(1.76)[1](d) | 1.768,1.759(1.78)[2*](d) | 1.812, 1.802(1.82)[3](d) | 1.800, 1.791(d) |
| 20 | 8.582 (8.58)[1](s) | 8.480(8.20)[2*](s) | 8.867 (8.81)[3](s) | 9.533 (9.77)[4**](s) |
| P1 | 4.342 (4.33)[1],4.224 (4.21)[1] | 4.364, 4.247 | 4.343 (4.26)[3], 4.227 (4.36)[3] | 4.361, 4.263 |
| P2 | 4.955 (4.95)[1] | 4.980 | 4.944 (5.04)[3] | 4.987 |
| P3 | - | - | - | - |
| P3[1] | 1.509 (1.51)[1] | 1.519 | 1.505 (1.54)[3] | 1.525 |
| P4 | 1.822 (1.82)[1] | 1.845 | 1.832 (1.85)[3] | 1.845 |
| P5 | 1.31 | 1.31 | 1.30 | 1.195 |
| P6 | 0.97,1.17 | 0.98,1.18 | 1.97,1.16 | 0.97,1.17 |
| P7 | 1.31 | 1.33 | 1.31 | 1.324 |
| P7[1] | 0.811,(0.81)[1], 0.803(0.80)[1] | 0.785, 0.777 | 0.778, 0.770 (0.79)[3] | 0.785, 0.777 |
| P8 | 1.01,1.23 | 1.02,1.22 | 1.01,1.22 | 1.01,1.22 |
| P9 | 1.15,1.28 | 1.15,1.28 | 1.14,1.28 | 1.15,1.27 |
| P10 | 1.01,1.23 | 1.02,1.22 | 1.01,1.22 | 1.01,1.22 |
| P11 | 1.31 | 1.32 | 1.32 | 1.32 |
| P11[1] | 0.783(0.79)[1],0.774 (0.78)[1] | 0.809,0.801 | 0.806, 0.797 (0.81)[3] | 0.807, 0.798 |
| P12 | 1.01,1.23 | 1.02,1.22 | 1.01,1.22 | 1.01,1.22 |
| P13 | 1.23,1.28 | 1.23,1.28 | 1.23,1.28 | 1.23,1.28 |
| P14 | 1.12 | 1.12 | 1.12 | 1.12 |
| P15 | 1.500 (1.50)[1] | 1.489 | 1.497 (1.51)[3] | 1.495 |
| P15[1] | 0.854(0.86)[1],0.845 (0.84)[1] | 0.851,0.842 | 0.850 (0.85)[3], 0.842 (0.85)[3] | 0.849, 0.841 |
| P16 | 0.854(0.86)[1],0.845 (0.84)[1] | 0.851,0.842 | 0.850 (0.85)[3], 0.842 (0.85)[3] | 0.849, 0.841 |

[1]Kobayashi et al. (2000), [2]Wu et al. (1985), [3]Miyashita et al. (1997), [4]Chen et al. (2010)

* in $CDCl_3$, **in $CD_2Cl_2$/$d_5$-pyridine(97/3, *v*/*v*)

**Table 2.** [1]H-chemcal shifts of Chls *a, b, d* and *f* in acetone-$d_6$ at 273K

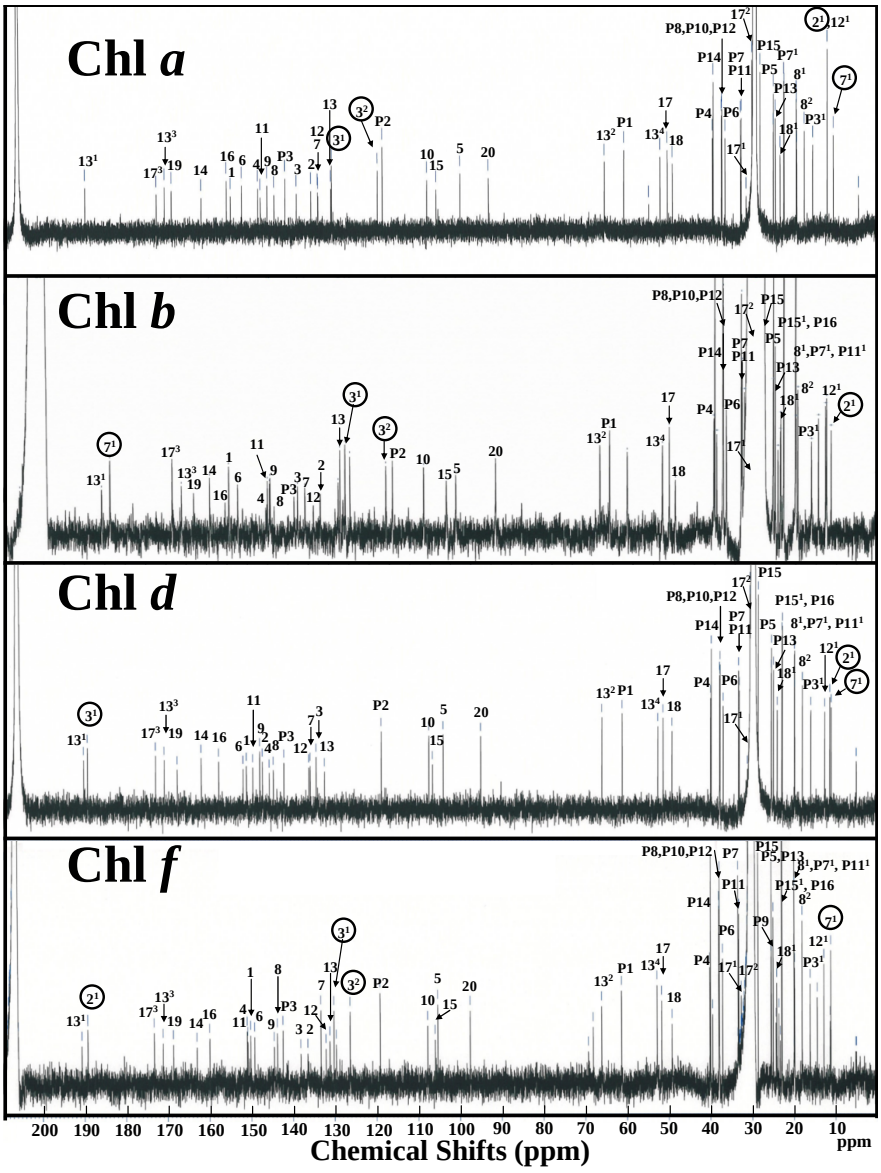


**Figure 12.** NMR spectra of Chls *a*, *b*, *d* and *f* measured in acetone-$d_6$ at 273 K. Signals corresponding to $^{13}C$ atoms of the molecules are labeled. The peak at 30-32 ppm is acetone.

http://dx.doi.org/10.5772/55460

| IUPAC no. of carbon atom | Chl *a* | Chl *b* | Chl *d* | Chl *f* |
|---|---|---|---|---|
| 1 | 155.47(155.46)[1] | 159.43 | 151.47(151.81)[2] | 151.02 |
| 2 | 136.28(136.24)[1] | 136.98 | 147.66(147.33)[2] | 136.49 |
| 2[1] | 12.65(12.70)[1] | 12.33 | 12.58(11.75)[2] | 189.27 |
| 3 | 139.76(139.68)[1] | 142.53 | 134.77(135.12)[2] | 138.17 |
| 3[1] | 131.30(131.29)[1] | 130.83 | 189.59(189.54)[2] | 130.22 |
| 3[2] | 120.33(120.33)[1] | 120.80 | - | 126.36 |
| 4 | 148.96(148.99)[1] | 150.15 | 146.00(146.36)[2] | 150.20 |
| 5 | 100.58(100.51)[1] | 103.63 | 106.24(104.41)[2] | 105.39 |
| 6 | 152.78(152.80)[1] | 157.25 | 152.27(152.55)[2] | 149.24 |
| 7 | 134.68(134.65)[1] | 140.76 | 136.19(136.31)[2] | 133.35 |
| 7[1] | 11.15(11.16)[1] | 188.62 | 11.25(11.39)[2] | 11.17 |
| 8 | 145.08(145.02)[1] | 148.32 | 145.02(145.13)[2] | 143.83 |
| 8[1] | 19.91(19.88)[1] | 19.51 | 19.94(20.12)[2] | 19.87 |
| 8[2] | 18.12(18.18)[1] | 19.91 | 18.12(18.12)[2] | 18.07 |
| 9 | 146.74(146.74)[1] | 149.29 | 148.28(148.64)[2] | 144.59 |
| 10 | 108.50(108.53)[1] | 111.53 | 107.68(107.8)[2] | 107.82 |
| 11 | 148.34(148.34)[1] | 149.94 | 149.97(150.35)[2] | 159.99 |
| 12 | 134.57(134.46)[1] | 138.66 | 136.50(136.63)[2] | 132.12 |
| 12[1] | 12.65(12.66)[1] | 12.47 | 12.79(12.89)[2] | 12.82 |
| 13 | 131.53(131.41)[1] | 132.13 | 132.76(133.04)[2] | 131.19 |
| 13[1] | 190.30(190.37)[1] | 190.66 | 190.49(190.50)[2] | 190.68 |
| 13[2] | 66.00(65.95)[1] | 65.77 | 66.19(66.47)[2] | 66.13 |
| 13[3] | 171.32(171.36)[1] | 171.04 | 171.20(171.33)[2] | 173.30 |
| 13[4] | 52.67(52.71)[1] | 52.79 | 52.79(52.84)[2] | 52.83 |
| 14 | 162.55(162.58)[1] | 164.11 | 162.30(162.68)[2] | 168.67 |
| 15 | 106.35(106.27)[1] | 105.94 | 106.82(107.04)[2] | 106.03 |
| 16 | 156.50(156.54)[1] | 160.38 | 158.12(158.60)[2] | 163.04 |
| 17 | 50.98(50.92)[1] | 51.14 | 51.54(52.05)[2] | 51.74 |
| 17[1] | 30.28(30.03)[1] | 30.28 | 30.66(30.64)[2] | 30.90 |
| 17[2] | 30.66(30.09)[1] | 30.66 | 31.27(31.37)[2] | 30.35 |
| 17[3] | 173.29(173.39)[1] | 173.35 | 173.26(173.45)[2] | 189.25 |
| 18 | 49.73(49.69)[1] | 49.65 | 49.44(49.80)[2] | 49.26 |
| 18[1] | 23.01(23.88)[1] | 23.68 | 24.13(24.25)[2] | 24.20 |
| 19 | 169.69(167.74)[1] | 168.03 | 168.09(168.34)[2] | 171.15 |
| 20 | 93.78(93.79)[1] | 93.86 | 95.26(95.36)[2] | 97.60 |
| P1 | 61.31(61.32)[1] | 61.42 | 61.33(61.67)[2] | 61.35 |
| P2 | 120.17(119.12)[1] | 119.19 | 119.13(119.53)[2] | 119.18 |
| P3 | 142.46(142.48)[1] | 143.42 | 142.49(142.70)[2] | 142.49 |
| P3[1] | 16.11(16.10)[1] | 16.16 | 16.11(16.40)[2] | 16.13 |
| P4 | 40.19(40.19)[1] | 40.23 | 40.19(40.46)[2] | 40.20 |
| P5 | 25.54(25.52)[1] | 25.57 | 25.53(25.86)[2] | 25.55 |
| P6 | 37.11 | 37.14 | 38.11(37.40)[2] | 37.11 |
| P7 | 33.43(33.44)[1] | 33.44 | 33.22(33.47)[2] | 33.50 |
| P7[1] | 20.03(20.02)[1] | 20.03 | 19.98(20.19)[2] | 20.02 |
| P8 | 37.94 | 37.95 | 37.94(38.21)[2] | 37.94 |
| P9 | 25.04(25.06)[1] | 25.06 | 25.04(25.25)[2] | 25.04 |
| P10 | 38.01 | 38.02 | 38.01(38.26)[2] | 38.01 |
| P11 | 33.22(33.23)[1] | 33.25 | 33.42(33.65)[2] | 33.42 |
| P11[1] | 19.98(19.98)[1] | 19.99 | 20.02(20.23)[2] | 19.98 |
| P12 | 37.87 | 37.89 | 37.88(38.14)[2] | 37.88 |
| P13 | 25.49(25.52)[1] | 25.49 | 25.49(25.64)[2] | 25.48 |
| P14 | 40.00(39.98)[1] | 40.00 | 40.00(40.27)[2] | 40.00 |
| P15 | 28.65(28.66)[1] | 28.65 | 28.65(28.85)[2] | 28.65 |
| P15[1] | 23.01[3] (28.66)[1] | 23.01[4] | 23.01[5] (23.15)[2] | 23.00[6] |
| P16 | 22.90[3] (22.91)[1] | 22.91[4] | 22.90[5] (23.07)[2] | 22.90[6] |

[1]Kobayashi et al. (2000), [2]Miyashita et al. (1997)

[3-6] assignment interchangeable

**Table 3.** $^{13}$C-chemcal shifts of Chls *a, b, d* and *f* in acetone-$d_6$ at 273K

The signals of $7^1$-$CH_3$ of Chls *a*, *d* and *f* show almost the same chemical shifts, 11.15 ppm, 11.24 ppm and 11.17 ppm, respectively, indicating the interaction between the -CHO and $7^1$-$CH_3$ moieties in Chls *d* and *f* are negligibly small, and hence the -CHO substituent is not so close to the $7^1$-$CH_3$ moiety in Chls *d* and *f*. The chemical shifts of $3^2$-vinyl carbons in Chls *a* and *b* are almost identical (120.3-120.8 ppm), but Chl *f* shows a slight but significant downfield shift (126.3 ppm), suggesting that the formyl substituent in Chl *f* is positioned very close to the 3-vinyl group, most probably on C2. The signals of -CHO moiety of Chls *d* and *f* exhibits almost the same chemical shift (189.59 ppm and 189.27 ppm), but a slight upfield C-formyl signal is observed at 188.62 ppm in Chl *b*, indicating that the environment of -CHO in Chls *d* and *f* is very similar, supporting that the -CHO moieties of Chls *d* and *f* are positioned at the same ring I, while that of Chl *b* is at ring II.

*3.5.3. NOESY*

Two-dimensional NMR spectra provide further information about a molecule than one-dimesional NMR spectra. NOESY is one of several types of two-dimensional NMR, where the nuclear Overhauser effect (NOE) between nuclear spins is used to establish the correlations. The cross-peaks in the two-dimensional spectrum connect resonances from spins that are spatially close to each other.

To obtain further evidence for the structural identity of Chl *f*, the signals were investigated using NOESY spectra. First of all, we had better see well-defined coherent correlations on the NOESY spectrum of Chl *a*. Here, we will trace the coherent correlations from meso-20-H, because Chl *f* posseses -CHO most probably at C2 near to C20. Coherent correlations can be easlily traced from 20-H on the NOESY spectrum of Chl *a* (Fig. 13), where the signal of 20-H at 8.582 ppm shows three cross peaks with the signals of $18^1$-H at 1.771 ppm, $2^1$-H at 3.343 ppm, and 18-H at 4.572 ppm. Good coherent correlations can also be traced from meso-5-H and meso-10-H; (1) the signal of 5-H at 9.410 ppm shows three cross peaks with the signal of $7^1$-H at 3.300 ppm, $3^2$-H at 6.242 ppm, and $3^1$-H at 8.162 ppm, and (2) the signal of 10-H at 9.749 ppm shows two cross peaks with the signal of $8^2$-H at 1.696 ppm and $12^1$-H at 3.619 ppm. In Chl *b* and Chl *d*, similar nice correlations are seen (Fig. 13).

To obtain further evidence for Chl *f*, a NOESY spectrum is illustrated in Fig. 13. As expected, nice coherent correlations can be traced from meso-20-H, the signal of 20-H at 9.553 ppm shows three cross peaks with the signal of 18-H at 4.634 ppm, $18^1$-H at 1.816 ppm, and $2^1$-H, most probably assigned to -CHO moiety, at 11.215 ppm. The signal of meso-5-H at 9.770 ppm shows three cross peaks with the signal of $7^1$-H at 3.351 ppm, $3^2$-H at 6.347 ppm, and $3^1$-H at 8.534 ppm. Similarly, coherent correlations of meso-10-H with $8^1$-H (3.754 ppm) and $12^1$-H (3.637 ppm) are clearly seen. These results indicate that the C-20 methine, among the three methines, is nearest to the -CHO moiety, supporting the substitution position by -CHO is most likely at C2 in Chl *f*.

http://dx.doi.org/10.5772/55460

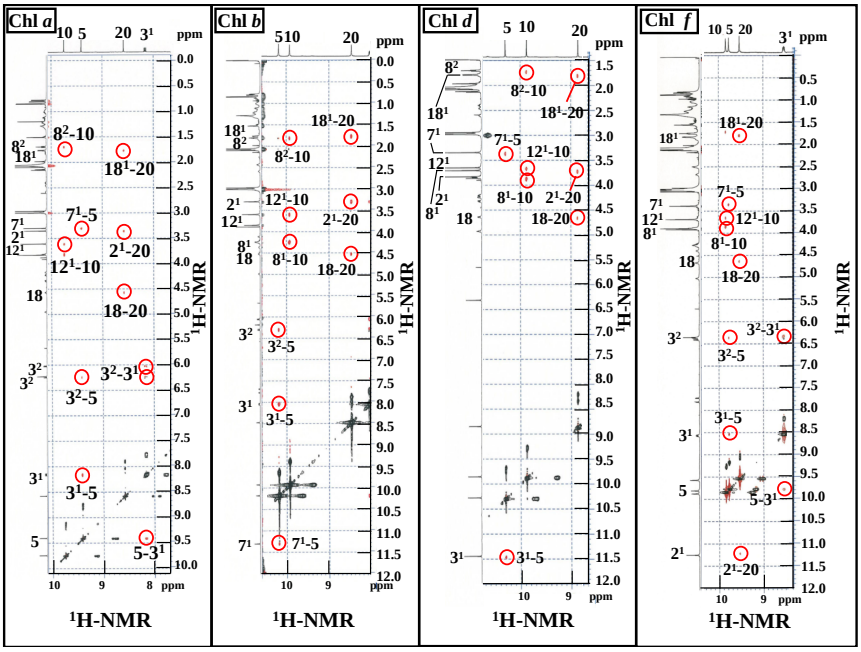


**Figure 13.** $^{1}$H-$^{1}$H-NOESY spectra of Chls *a*, *b*, *d* and *f* measured in acetone-$d_6$ at 273 K.

### *3.5.4. HSQC*

HSQC is a two-dimensional inverse correlation technique that allows for the determination of connectivity between two different nuclear species, and HSQC is selective for direct coupling. As illustrated in the $^{1}$H-$^{13}$C HSQC spectra of Chls *a*, *b*, *d* and *f* (Fig. 14), all substituents on the macrocycle show the corresponding cross peaks. The results support that one methyl group of Chl *a* is replaced with a formyl one in Chl *f*.

### *3.5.5. HMBC*

HMBC is also a two-dimensional inverse correlation method that allows for the determination of connectivity between two different nuclear species like HSQC, but HMBC gives longer range coupling (2-4 bond coupling) than HSQC.

Three meso-Hs in Chl *a* exhibit one to three cross peaks as seen in Fig. 15A. The formyl-H in Chls *b*, *d* and *f* shows two to four cross peaks. For example, in the $^{1}$H-$^{13}$C HMBC spectrum of Chl *f*, the $^{1}$H-signal for 2$^{1}$-CHO has four cross peaks, one is with the signal for 3$^{1}$-vinylic carbons, one is with the signal for 1C carbon, and the other two are with the signal for 2$^{1}$-CHO carbon, where the cross peak split is due to the direct coupling. Conclusively, the Chl *f*-like pigment isolated from the strain KC1 has been identified as Chl *f*, namely, 2-desmethyl-2-formyl-Chl *a* ([2-CHO]-Chl *a*).

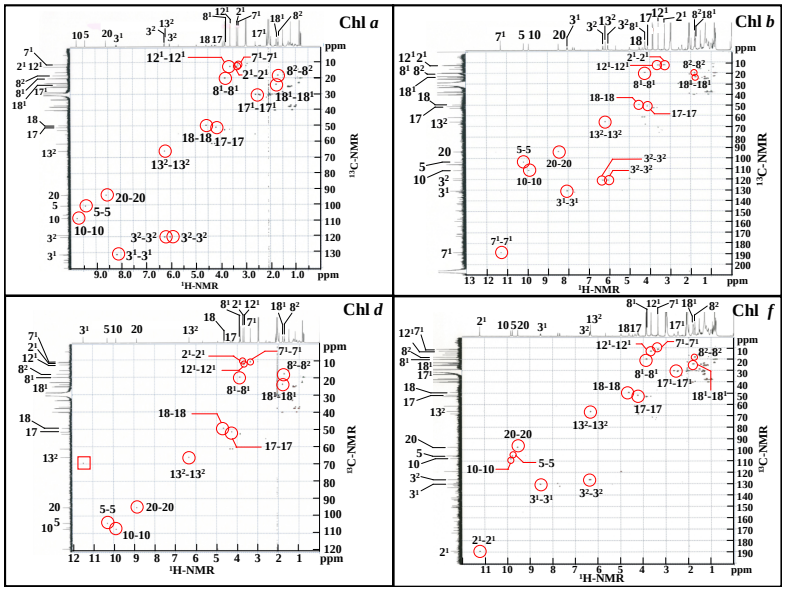


**Figure 14.** $^{1}H$-$^{13}C$-HSQC spectra of Chls *a*, *b*, *d* and *f* measured in acetone-$d_6$ at 273 K. □ in Chl *d*: δC189.59 (folded from outside the spectral window)

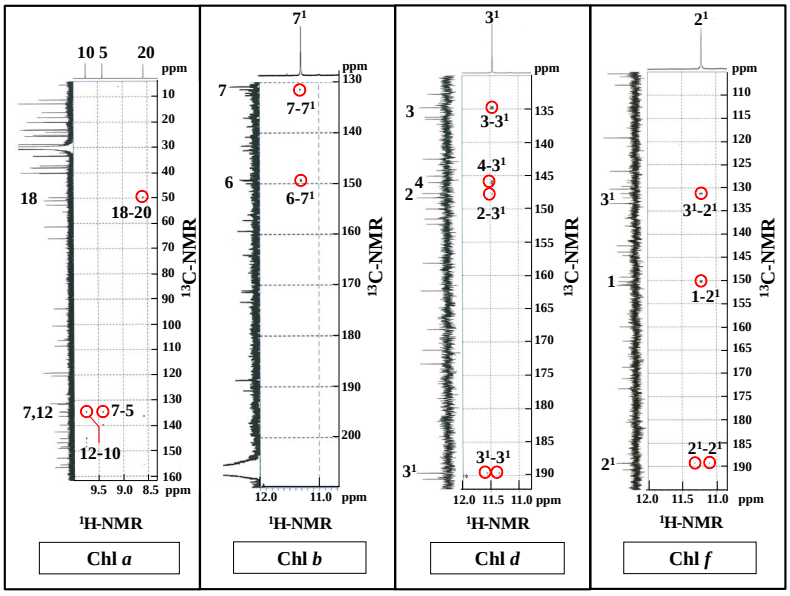


**Figure 15.** $^{1}H$-$^{13}C$-HMBC spectra of Chls *a*, *b*, *d* and *f* measured in acetone-$d_6$ at 273 K.

http://dx.doi.org/10.5772/55460

### 3.6. Redox potentials

To understand the charge separation in the RC, electrochemical characterization of chlorophylls is of crucial importance. In this section, the redox potentials of Chls and Phes *in vitro* are presented.

Acetonitrile (Aldrich, anhydrous grade: water < 50 ppm) was deoxygenated and dried before use. The solvent was subjected to freeze-pump-thaw cycles at least three times under about $10^{-5}$ torr. Under a nitrogen atmosphere, the deoxidized solvent was then dried for 24 h with activated molecular sieves (4A 1/16, Wako), pretreated *in vacuo* at 473 K over 24 h. Tetra-*n*-butylammonium perchlorate ($Bu_4NClO_4$, TBAP) (Aldrich, Electrochemical grade: > 99.0 %), was used as the supporting electrolyte, which had been recrystallized from methanol solution and then dried in vacuo at 333 K over 24 h.

The redox potentials of chlorophylls were measured by square wave voltammetry (SWV). The signal-to-noise ratio of SWV is generally better than that of CV, especially for measuring redox couples at such low concentration (ca. 0.5 mM) as in the present case (Cotton et al. 1979, Wasielewski et al. 1980). Measurements were done with an ALS model 620A electrochemical analyzer. Parameters for SWV were $V_{step}$ = 5.0 mV, AC signal ($V_{pulse}$) = 25 mV, and p-p at 8 Hz. The measurements were carried out in an air-tight electrochemical cell containing a small compartment for a sample solution (ca. 0.5 mM) equipped with a glass filter that can be degassed and filled with dry $N_2$. A platinum disk electrode with 1.6 mm in diameter (outer diameter: 3 mm) was used as the working electrode, and a platinum black wire fabricated in the small compartment (internal diameter: 8.9 mm) as the counter electrode. An Ag/AgCl electrode, chosen for good reproducibility despite possibility of junction potential, was connected through a salt bridge to the outer electrolytic solution of the small components. After measurement, the redox potentials of the ferrocene-ferrocinium were measured as +0.45 V vs. Ag/AgCl in acetonitrile.

Typical square wave voltammograms (SWVs) for Chls *a*, *b*, *d* and *f* in acetonitrile are illustrated in Fig. 16. Four peaks are observed in each voltammogram and the potentials in anodic sweep and cathodic sweep (data not shown) are identical to each other, indicating that the four redox reactions are reversible. Similar trends are observed for Phes *a*, *b* and *d* (data not shown). The measurement for Phe *f* is now underway.

In Table 4 are summarized the redox potentials for Chls *a*, *b*, *d*, *f*, Phes *a*, *b* and *d*. Chl *d* shows higher oxidation potentials than Chl *a*, lower than Chl *b*, and much lower than Phe *a*, Phe *b* and Phe *d*. Chl *f* exhibits higher oxidation potentials than Chls *a*, *d*, and lower than Chl *b*. The results can be explained by invoking the inductive effect of substituent groups on the macrocycle, because the redox potentials of chlorophylls are sensibly affected by the nature of substituent groups on the π-electron system (Fuhrhop 1975, Watanabe and Kobayashi 1991, Kobayashi et al. 2007).

The -CHO substituent on Chls *b*, *d* and *f* is an electron-withdrawing group (→CHO), and hence reduces the electronic density in the π-system of chlorophyll. The replacements of $-CH_3$ at C7 or C2 of Chl *a* by →CHO to yield Chl *b* or Chl *f* cause the macrocycle to be electron poor, thus

rendering the molecule less oxidizable ($E^1_{ox}$: Chl *b*, *f* > Chl *a*). Similarly, replacement of -CH=$CH_2$ at C3 of Chl *a* by →CHO to yield Chl *d* makes the first oxidation potential, $E^1_{ox}$, more positive than that of Chl *a* ($E^1_{ox}$: Chl *d* > Chl *a*). Therefore, the $E^1_{ox}$ order becomes Chls *b*, *d*, *f* > Chl *a* (see Figs 16 and 17). When one pays attention to the group of -$CH_3$ at C7 of Chl *d* and the group of -CH=$CH_2$ at C3 of Chl *b* or C7 of Chl *f*, the -$CH_3$ group is more electron-donating (←$CH_3$), thus making the macrocycle of Chl *d* more electron rich, and hence its oxidation potential less positive (Chls *b*, *f* > *d*); the $E^1_{ox}$ order results in Chls *b*, *f* > Chl *d* > Chl *a*. As expected from the inductive effect of substituent groups, Chls *b* and *f* show the almost the same $E^1_{ox}$ values. Consequently, as seen in Fig. 17, the $E^1_{ox}$ order results in Chl *b* > Chl *f* > Chl *d* > Chl *a*; a little higher oxidation potential of Chl *b* than that of Chl *f*, 20 mV, cannot be explained from the primitive way used here.

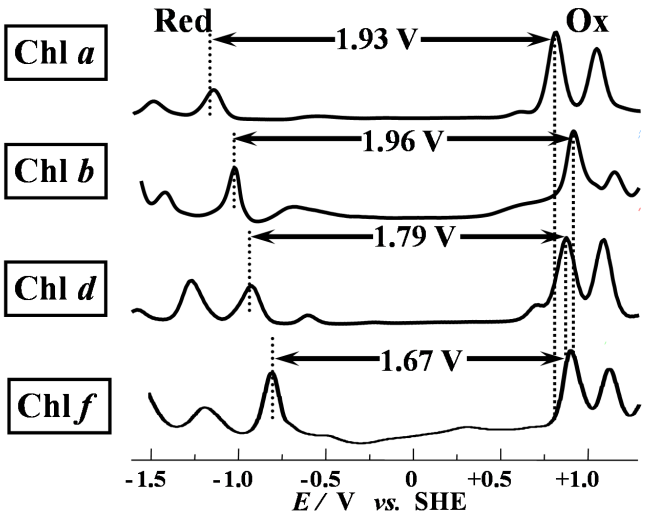


**Figure 16.** Square wave voltammograms of Chls *a*, *b*, *d* and *f* in acetonitrile.

| | $E^2_{red}$ | $E^1_{red}$ | $E^1_{ox}$ | $E^2_{ox}$ | $E^1_{ox} - E^1_{red}$ |
|---|---|---|---|---|---|
| | | | V vs. SHE | | |
| Chl *a* | -1.46 | -1.12 | 0.81 | 1.04 | 1.93 |
| Chl *b* | -1.41 | -1.02 | 0.94 | 1.15 | 1.96 |
| Chl *d* | -1.27 | -0.91 | 0.88 | 1.09 | 1.79 |
| Chl *f* | -1.12 | -0.75 | 0.92 | 1.13 | 1.67 |
| Phe *a* | -1.00 | -0.75 | 1.14 | 1.49 | 1.89 |
| Phe *b* | -1.05 | -0.64 | 1.25 | 1.58 | 1.89 |
| Phe *d* | -0.87 | -0.63 | 1.21 | 1.50 | 1.84 |

**Table 4.** Redox potentials of Chls *a*, *b*, *d*, *f*, Phes *a*, *b* and *d* in acetonitrile

http://dx.doi.org/10.5772/55460

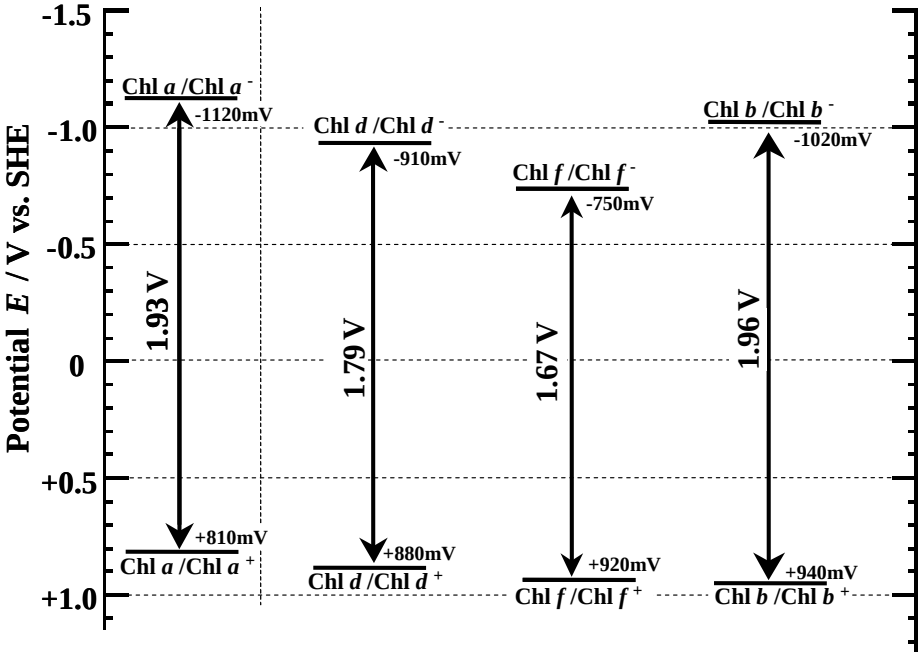


**Figure 17.** Schematic comparison of redox potentials of Chls *a*, *b*, *d* and *f* in acetonitrile.

The redox behavior of a compound is related to the energy levels of its molecular orbitals: $E^1_{ox}$ is intimately related to the highest occupied molecular orbital (HOMO) and $E^1_{red}$ to the lowest unoccupied molecular orbital (Watanabe and Kobayashi 1991; Hanson 1991). The order of HOMO energy levels well parallels the $E^1_{ox}$ values, while the correlation between the LUMO levels and the $E^1_{red}$ values is less conspicuous (see Fig. 7 in Watanabe and Kobayashi 1991).

As clearly seen in Fig. 17, the order of absolute values of the first reduction potentials, $E^1_{red}$, of Chls *a*, *d* and *f* is Chl *a* > Chl *d* > Chl *f*, which can be well explained by substituent inductive effect, like $E^1_{ox}$ as mentioned above. This simple rule, however, does not hold for Chls *d* and *f*; their values of $E^1_{red}$ are remarkably more positive than those of Chls *a* and *b*; compared to Chl *a*, Chl *b* is harder to oxidize by 130 mV, and easier to reduce by 100 mV, namely, similar in degree, while Chls *d* and *f* peculiarly easier to reduce by 210 mV and 370 mV. The findings indicate that the inductive effect of substituent groups at ring II conspicuously appears for $E^1_{red}$. Anyway, this irregularity may come from the fact that the LUMO energy levels are to a lesser extent correlated with the $E^1_{red}$ values.

The primary redox potential difference, $\Delta E = E^1_{ox} - E^1_{red}$, seen in Fig. 17 can be taken as an index for the $Q_Y$ excitation energy (Watanabe and Kobayashi 1991; Hanson 1991). For example, $\Delta E$ for Chl *a* is 1.93 eV in Fig. 17, which corresponds to the $Q_Y$ excitation wavelengths to a certain extent, 661-666 nm for Chl *a* in Fig.17. Similarly. $\Delta E$ = 1.96 eV, 1.79 eV and 1.67 eV for Chls *b*,

*d* and *f* also correlate to the $Q_Y$ wavelengths, 644-662 nm, 686-698 nm. and 695-708 nm. Pheophytins also behave in a similar fashion.

In 1959, the domination of inductive effects of the central metal over a conjugative macrocycle has first been formulated (Gouterman 1959). The redox potential of chlorophyll shows a systematic shifts with the electronegativity of the central metal, and such a trend is rationalized in terms of an electron density decrease in the chlorin $\pi$-system by the presence of an electron negative metal in the center of chlorophylls (Watanabe and Kobayashi 1991; Hanson 1991; Noy et al. 1998). Inspection of Table 4 demonstrates that such a trend is essential for the pair of Chls and Phes; the electronegativity of 2.2 for H is significantly higher than that of 1.2 for Mg, which renders Phes more difficult to oxidize than the corresponding Chls.

## 4. Evolutionary and ecological aspects of chlorophylls

### 4.1. Diversification of chlorophylls during the evolution of photosynthetic organisms

Chlorophylls are distributed among oxygenic photosynthetic organisms, including cyanobacteria, algae and terrestrial plants (Falkowski et al. 2004). It is generally accepted that plastids first arose by endosymbiosis between photosynthetic prokaryotes (ancestral to present cyanobacteria) and non-photosynthetic eukaryotic hosts (Fig. 18). There are two different types of hypothesis for the evolution of Chl *b*. One is based on vertical transfer of the gene for Chl *b* biosynthesis, which includes the lost of the gene. The other is based on the lateral gene transfer for Chl *b* biosynthesis. In the hypothesis of the former one, the ancestral cyanobacteria contained both Chls *a* and *b*, and the gene for Chl *b* biosynthesis had been lost. In many cyanobacterial linage as well as the linages of the red algae and glaucophytes, the gene had been lost, whereas a few linage of cyanobacteria, (*Prochloron* and *Prochlorothrix*) and the green algae (and terrestrial plants) retained it. This hypothesis is partly supported by the high homology of the enzyme for Chl *b* biosynthesis (CAO) (Tomitani et al. 1999). In the latter hypothesis, the gene for Chl *b* biosynthesis was firstly evolved in the ancestor of green algae or cyanobacteria, and the gene was transferred into different linages. This is supported by the fact that one gene transfer was enough for the acquisition of Chl *b* biosynthesis in cyanobacerium. The secondary endosymbioses of green algae gave rise to euglenophytes, chlorarachniophytes and "green" dinoflagellates, which were containing Chls *a* and *b*. The secondary or tertiary plastids of cryptophytes, haptophytes, heterokonts and dinoflagellates contain Chl *c* in addition to Chl *a*. Most of present-day cyanobacteria contain only Chl *a*, and only a few genera are known to keep Chl *b* (*Prochloron* and *Prochlorothrix*). This suggests that Chl *b* had been lost in polyphyletic lineage during the evolution of cyanobacteria. Some cyanobacteria contain divinyl chlorophylls (DVChls) *a* and *b* (*Prochlorococcus*), Chl *d* (*Acaryochloris*) and Chl *f* (strain KC1 and *Halomicronema hongdechloris*). These chlorophylls are only found in cyanobacteria, and it has yet to be revealed when and how they acquired these pigments.

http://dx.doi.org/10.5772/55460

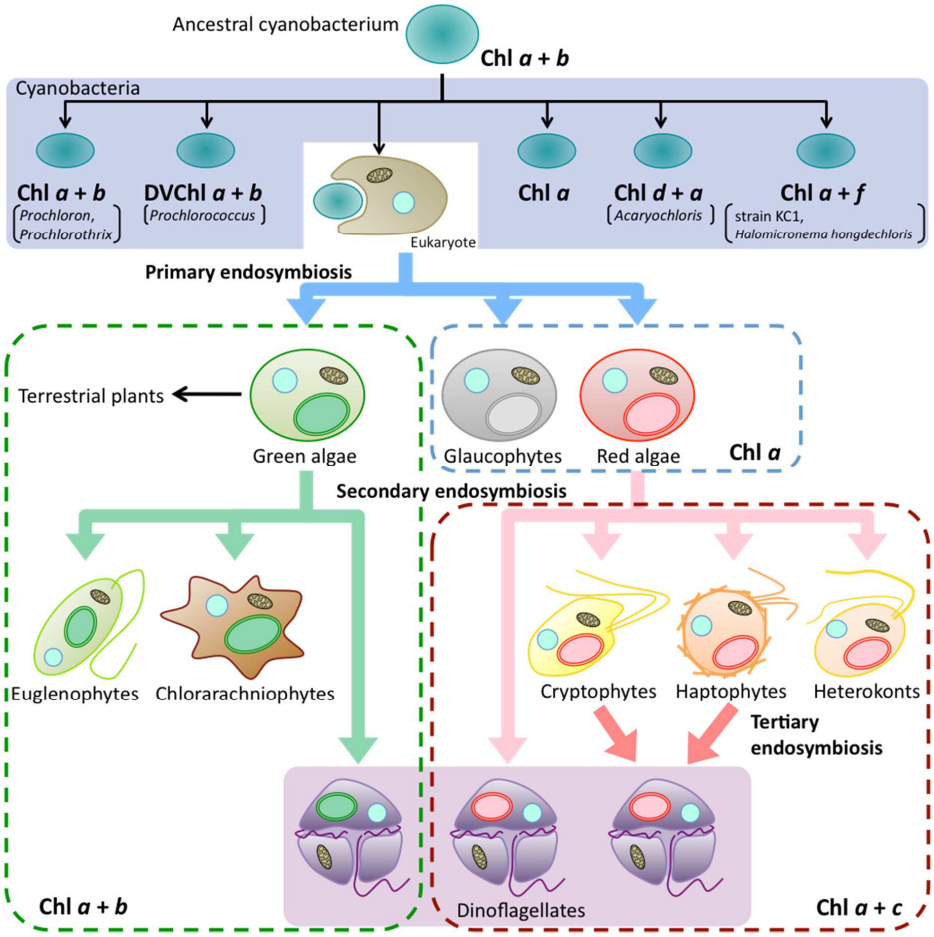


**Figure 18.** The distribution of various chlorophylls among oxygenic photosynthetic organisms.

### 4.2. Ecology of the red-shifted chlorophylls

Acquisition of new or additional chlorophylls by photosynthetic organisms is thought to be an adaptation to the light quality of their niches. The two red-shifted chlorophylls, Chls *d* and *f*, are also thought be acquired and selected by a part of cyanobacteria for their growth and survival by sustaining oxygenic photosynthesis using the light available at their niches.

Chl *d*-containing cyanobacterium, *Acaryochloris marina*, was firstly found as a minor symbionts in colonial ascidians which had large numbers of cyanobacterial symbionts, *Prochloron*, which

contain Chls *a* and *b* as their photosynthetic chlorophylls (Miyashita et al. 1996). Subsequently, *Acaryochloris* spp. has been found on the surface of coastal macroalgae (Murakami et al. 2004), under those colonial ascidians (Kühl et al. 2005), and in coastal microbial mats at a saline lake (Miller et al. 2005). In all of those niches, *Acaryochloris* spp. competes for light for their oxygenic photosynthesis. However, due to the possession of Chl *d* as primary chlorophyll, *Acaryochloris* spp. can absorb and utilized far-red light from 700 nm to 740 nm for oxygenic photosynthesis (Miyashita et al. 1997). The ability has advantage for their growth and survival, since another oxygenic phototrophs which contain Chl *a* as their primary chlorophyll cannot absorb and utilize the light.

Chl *f*-containing cyanobacterium was firstly reported in microbial mat, where the competition for the light also occurs among the phototrophs (Chen et al. 2010). While the distribution and detailed niche of Chl *f*-containing cyanobacteria have not been elucidated yet, Chl *f* must contribute to the survival of those cyanobacteria. Since Chl *f* in cyanobacteria also absorbed far-red light around 720 nm and Chl *f*-possessing cyanobacteria can grow under far-red LED light as a sole light source (Chen and Blankenship 2011).

## Acknowledgements

We thank Dr. Nobuaki Ishida (Ishikawa Prefectural Univ.), Dr. Yoshihiro Shiraiwa and Dr. Koji Iwamoto (Univ. Tsukuba) for their invaluable help. This work was supported in part by Special Project of Organization for the Support and Development of Strategic Initiatives (Green Innovation) (Univ. Tsukuba) to M.K.

## Author details

Masami Kobayashi[1], Shinya Akutsu[1], Daiki Fujinuma[1], Hayato Furukawa[1], Hirohisa Komatsu[1], Yuichi Hotota[1], Yuki Kato[2], Yoshinori Kuroiwa[2], Tadashi Watanabe[3], Mayumi Ohnishi-Kameyama[4], Hiroshi Ono[4], Satoshi Ohkubo[5] and Hideaki Miyashita[5]

1 Institute of Materials Science, University of Tsukuba, Tsukuba, Japan

2 Institute of Industrial Science, University of Tokyo, Tokyo, Japan

3 Research Center for Math and Science Education, Organization for Advanced Education, Tokyo University of Science, Tokyo, Japan

4 National Food Research Institute, Tsukuba, Japan

5 Graduate School of Human and Environmental Studies, Kyoto University, Kyoto, Japan

http://dx.doi.org/10.5772/55460

## References

[1] Akiyama M, Miyashita H, Kise H, Watanabe T, Miyachi S and Kobayashi M (2001) Detection of chlorophyll d' and pheophytin a in a chlorophyll d-dominating oxygenic photosynthetic prokaryote Acaryochloris marina. Anal. Sci. 17: 205-208

[2] Akiyama M, Miyashita H, Kise H, Watanabe T, Mimuro M, Miyachi S and Kobayashi M (2002) Quest for minor but key chlorophyll molecules in photosynthetic reaction centers - Unusual pigment composition in the reaction centers of a chlorophyll d-dominated cyanobacterium Acaryochloris marina -. Photosynth. Res. 74: 97-107

[3] Akiyama M, Gotoh T, Kise H, Miyashita H, Mimuro M and Kobayashi M (2004) Stoichiometries of chlorophyll d'/PSI and chlorophyll a/PSII in a chlorophyll d-dominated cyanobacterium Acaryochloris marina. Jpn. J. Phycol. (Supplement for the Proceedings of Algae 2002) 52:67-72

[4] Akutsu S, Fujinuma D, Furukawa H, Watanabe T, Ohnishi-Kameyama M, Ono H, Ohkubo S, Miyashita H and Kobayashi M (2011) Pigment analysis of a chlorophyll f-containing cyanobacterium strain KC1 isolated from Lake Biwa. Photomed. Photobiol. 33: 35-40

[5] Behrendt L, WD Larkum A, Norman A, Qvortrup K, Chen M, Ralph P J, Sørensen S, Trampe E and Ku°hl M (2011) Endolithic chlorophyll d containing phototrophs. ISME J. 5: 1072-1076

[6] Benjamin B, Finazzi G, Benson S, Barber J, Rappaport F and Telfer A (2007) Study of intersystem electron transfer in the chlorophyll d containing cyanobacterium Acaryochloris marina and a reappraisal of the redox properties of P740. Photosynth. Res. 91:155

[7] Boomer SM, Pierson BK, Austinhirst R and Castenholz RW (2000) Characterization of novel bacteriochlorophyll-a-containing red filaments from alkaline hot springs in Yellowstone National Park. Arch. Microbiol. 174: 152-161

[8] Brettel K (1997) Electron transfer and arrangement of the redox cofactors in photosystem I. Biochim. Biophys. Acta 1318: 322-373

[9] Chen M, Schliep M, Willows RD, Cai Z, Neilan BA and Scheer H (2010) A red-shifted chlorophyll. Science 329: 1318-1319

[10] Chen M and Blankenship R E. (2011) Expanding the solar spectrum used by photosynthesis. Trends in Plant Science 16: 427-431

[11] Chen M, Li Y, Birch D and Willows RD (2012) A cyanobacterium that contains chlorophyll f – a red-absorbing photopigment. FEBS Lett. 586: 3249-3254

[12] Cotton TM and Van Duyne RP (1979) Electrochemical investigation of the redox properties of bacteriochlorophyll and bacteriopheophytin in appoticsolvents, J. Am. Chem. Soc. 101: 7605–7612.

[13] Eskins K Scholfield CR and Dutton HJ (1977) High-performance liquid chromatography of plant pigments. J. Chromatogr. 135: 217-220.

[14] Falkowski PG, Katz ME, Knoll AH, Quigg A, Raven JA, Schofield O and Taylor FJR (2004) The evolution of modern eukaryotic phytoplankton, Science 305: 354.

[15] Fajer J, Brune DC, Davis MS, Forman A and Spaulding LD (1975) Primary charge separation in bacterial photosynthesis: Oxidized chlorophylls and reduced pheophytin. Proc. Natl. Acad. Sci. USA 72: 4956-4960

[16] Fuhrhop JH (1975) Reversible reactions of porphyrins and metalloporphyrins and electrochemistry, in: Smith K.M. (ed.), Porphyrins and Metalloporphyrins. Elsevier, Amsterdam p. 14.

[17] Gouterman M (1959) Study of the effects of substitution on the absorption spectra of porphin. J. Chem. Phys. 30: 1139-1161

[18] Gouterman M (1961) Spectra of porphyrins. J. Mol. Spectrosc. 6: 138-163.

[19] Gouterman M, Wagniere G.H and Snyder LC (1963) Spectra of porphyrins part II. Four orbital model, J. Mol. Spectrosc. 11: 108-127

[20] Hanson LK (1991) Molecular orbital theory on monomer pigments. in: H. Scheer (ed.), Chlorophylls, CRC Press, Boca Raton. 993-1014.

[21] Hu Q, Miyashita H, Iwasaki I, Kurano N, Miyachi S, Iwaki M and Itoh S (1998) A photosystem I reaction center driven by chlorophyll d in oxygenic photosynthesis. Proc. Natl. Acad. Sci. USA 95: 13319-13323

[22] Hunt JE and Michalski TJ (1991) Desorption-ionization mass spectrometry of chlorophylls. In: Scheer H (ed) Chlorophylls, pp 835-853. CRC Press, Boca Raton

[23] Iriyama K, Yoshlura M and Shiraki M (1978) Micro-method for the qualitative and quantitative analysis of photosynthetic pigments using high-performance liquid chromatography. J. Chromatogr. 154: 302-305.

[24] Itoh S, Iwaki M, Noguti T, Kawamori A, Mino H, Hu Q, Iwasaki I, Miyashita H, Kurano KN, Miyachi S and Shen R (2001) Photosystem I and II reaction centers of a new oxygenic organism Acaryochloris marina that use chlorophyll. In: PS2001: Proceedings of the 12th International Congress on Photosynthesis, S6-028. CSIRO Publishing, Melbourne (CD-ROM)

[25] Itoh S, Mino H, Itoh K, Shigenaga T, Uzumaki T and Iwaki M (2007) Function of chlorophyll d in reaction centers of photosystems I and II of the oxygenic photosynthesis of Acaryochloris marina. Biochemistry 46:12473-12481.

[26] Jordan P, Fromme P, Witt HT, Klukas O, Saenger W, Krauβ N (2001) Three-dimensional structure of cyanobacterial photosystem I at 2.5 Å resolution. Nature 411: 909-917

[27] Kashiyama Y, Miyashita H, Ogawa NO, Chikaraishi Y, Takano Y, Suga H, Toyofuku T, Nomaki H, Kitazato H, Nagata T, and Ohkouchi N (2008) Evidence of global chlorophyll d. Science 321: 658

[28] Kaufmann KJ, Dutton PL, Netzel TL, Leigh JS and Rentzepis PM (1975) Picosecond kinetics of events leading to reaction center bacteriochlorophyll oxidation. Science 188: 1301-1304

[29] Ke B (2001) The primary electron donor of photosystem I-P700. in Photosynthesis. Photobiochemistry and Photobiophysics. pp. 463-477, Kluwer Academic Publishers, Dordrecht

[30] Kirmaier C, Blankenship RE and Holten D (1986) Formation and decay of radical-pair P+I- in Chloroflexus aurantiacus reaction centers. Biochim. Biophys. Acta 850: 275-285

[31] Klimov VV, Klevanik AV, Shuvalov VA and Krasnovsky AA (1977a) Reduction of pheophytin in the primary light reaction of photosystem II. FEBS Lett. 82: 183-186

[32] Klimov VV, Allkhverdiev SI, Demeter S and Krasnovsky AA (1977b) Photoreduction of pheophytin in photosystem 2 of chloroplasts with respect to the redox potential of the medium. Dokl. Akad. Nauk SSSR 249: 227-230

[33] Klimov VV, Shuvalov VA, Krakhmaleva IN, Klevanik AV and Krasnovskii AA (1977c) Photoreduction of bacteriopheophytin b in the primary light reaction of Rhodopseudomonas viridis chromatophores. Biokhimiya 42: 519-530

[34] Kobayashi M, Watanabe T, Nakazato M, Ikegami I, Hiyama T, Matsunaga T and Murata N (1988) Chlorophyll a'/P700 and pheophytin a/P680 stoichiometries in higher plants and cyanobacteria determined by HPLC analysis. Biochim. Biophys. Acta 936: 81-89

[35] Kobayashi M, van de Meent EJ, Amesz J, Ikegami I and Watanabe T (1991) Bacteriochlorophyll g epimer as a possible reaction center component of heliobacteria. Biochim. Biophys. Acta 1057: 89-96

[36] Kobayashi M, van de Meent EJ, Oh-oka H, Inoue K, Itoh S, Amesz J and Watanabe T (1992) Pigment composition of heliobacteria and green sulfur bacteria. In: Murata N (ed) Research in Photosynthesis, Vol 1, pp 393-396. Kluwer Academic Publishers, Dordrecht

[37] Kobayashi M, Akiyama M, Yamamura M, Kise H, Ishida N, Koizumi M, Kano H and Watanabe T (1998a) Acidiphilium rubrum and zinc-bacteriochlorophyll, part2: Physicochemical comparison zinc-type chlorophylls and other metallochloro-phylls. in

Photosynthesis: Mechanism and Effects, ed. by Garab, G., Kluwer Academic Publishers, Dordrecht, The Netherlands, vol. 2, 735-738

[38] Kobayashi M, Hamano T, Akiyama M, Watanabe T, Inoue K, Oh-oka H, Amesz J, Yamamura M and Kise H (1998b) Light-independent isomerization of bacteriochlorophyll g to chlorophyll a catalyzed by weak acid in vitro. Anal. Chim. Acta 365: 199-203

[39] Kobayashi M, Akiyama M, Kise H, Takaichi S, Watanabe T, Shimada K, Iwaki M, Itoh S, Ishida N, Koizumi M, Kano H, Wakao N and Hiraishi A (1998c) Structural determination of the novel Zn-containing bacteriochlorophyll in Acidiphilium rubrum. Photomed. Photobiol. 20: 75-80

[40] Kobayashi M, Yamamura M, Akutsu S, Miyake J, Hara M, Akiyama M and Kise H (1998d) Successfully controlled isomerization and pheophytinization of bacteriochlorophyll b by weak acid in the dark in vitro. Anal. Chim. Acta 361: 285-290

[41] Kobayashi M, Yamamura M, Akiyama M, Kise H, Inoue K, Hara M, Wakao N, Yahara K and Watanabe T (1998e) Acid resistance of Zn-bacteriochlorophyll a from an acidophilic bacterium Acidiphilium rubrum. Anal. Sci. 14: 1149-1152

[42] Kobayashi M, Oh-oka H, Akutsu S, Akiyama M, Tominaga K, Kise H, Nishida F, Watanabe T, Amesz J, Koizumi M, Ishida N and Kano H (2000) The primary electron acceptor of green sulfur bacteria, bacteriochlorophyll 663, is chlorophyll a esterified with Δ2,6-phytadienol. Photosynth. Res. 63: 269-280

[43] Kobayashi M, Watanabe S, Gotoh T, Koizumi H, Itoh Y, Akiyama M, Shiraiwa Y, Tsuchiya T, Miyashita H, Mimuro M, Yamashita T and Watanabe T (2005) Minor but key chlorophylls in Photosystem II. Photosynth. Res. 84:201-207

[44] Kobayashi M, Akiyama M, Kise H, Watanabe T (2006) Unusual tetrapyrrole pigments of photosynthetic antennas and reaction centers: Specially-tailored chlorophylls, Chlorophylls and Bacteriochlorophylls: Biochemistry, Biophysics, Functions and Applications, ed. by B. Grimm, R. J. Porra, W. Rüdiger and H. Scheer, Springer, Dordrecht, 55-66

[45] Kobayashi M, Akiyama M, Kano H, Kise H (2006) Spectroscopy and structure determination, in Chlorophylls and Bacteriochlorophylls: Biochemistry, Biophysics, Functions and Applications, ed. by B. Grimm, R. J. Porra, W. Rüdiger and H. Scheer, Springer, Dordrecht, 79-94

[46] Kobayashi M, Ohashi S, Iwamoto K, Shiraiwa Y, Kato Y, Watanabe T (2007) Redox potential of chlorophyll d in vitro. Biochim. Biophys. Acta 1767:596–602.

[47] Koizumi H, Itoh Y, Hosoda S, Akiyama M, Hoshino T, Shiraiwa Y, Kobayashi M (2005) Serendipitous discovery of Chl d formation from Chl a with papain, Sci. Tech. Adv. Material 6: 551–557.

[48] Krabben L, Schlodder E, Jordan R, Carbonera D, Giacometti G, Lee H, Webber A.N, Lubitz W (2000) Influence of the axial ligands on the spectral properties of P700 of photosystem I: a study of site-directed mutants. Biochemistry 39: 13012–13025

[49] Kühl M, Chen M, Ralph PJ, Schreiber U and Larkum AWD (2005) A niche for cyanobacteria containing chlorophyll d. Nature 433: 820

[50] Kumazaki S, Abiko K, Ikegami I, Iwaki M and Itoh S (2002) Energy equilibration and primary charge separation in chlorophyll d-based photosystem I reaction center isolated from Acaryochloris marina. FEBS Lett. 530:153-157

[51] Manning WM and Strain HH (1943) Chlorophyll d, a green pigment of red algae. J. Biol. Chem. 151: 1-19

[52] Miller SM, Augustine S, Olson TL, Blankenship RE, Selker J and Wood AM (2005) Discovery of a free-living chlorophyll d-producing cyanobacterium with a hybrid proteobacterial/cyanobacterial small-subunit rRNA gene. Proc. Natl. Acad. Sci. USA 102: 850–855.

[53] Miyashita H, Ikemoto H, Kurano N, Adachi K, Chihara M and Miyachi S (1996) Chlorophyll d as a major pigment. Nature 383: 402

[54] Miyashita H, Adachi K, Kurano N, Ikemoto H, Chihara M, Miyachi S (1997) Pigment composition of a novel oxygenic photosynthetic prokaryote containing chlorophyll d as the major chlorophyll. Plant Cell Physiol. 38:274-281

[55] Mohr R, Voss B, Schliep M, Kurz T, Maldener I and Adams DG (2010). A new chlorophyll d-containing cyanobacterium: evidence for niche adaptation in the genus Acaryochloris. ISME J. 4: 1456-1469.

[56] Murakami A, Miyashita H, Iseki M, Adachi K and Mimuro M (2004) Chlorophyll d in an epiphytic cyanobacterium of red algae. Science 303:1633.

[57] Nakamura A, Suzawa T and Watanabe T (2004) Spectroelectrochemical determination of the redox potential of P700 in spinach with an optically transparent thin-layer electrode. Chem. Lett. 33: 688-689.

[58] Noy D, Fiedor L, Hartwich G, Scheer H and Scherz A (1998) Metal-substituted bacteriochlorophylls. 2. Changes in redox potentials and electronic transition energies are dominated by intramolecular electrostatic interactions. J. Am. Chem. Soc. 120: 3684-3693

[59] Ohashi S, Miyashita H, Okada N, Iemura T, Watanabe T and Kobayashi M (2008) Unique photosystems in Acaryochloris marina. Photosynth. Res. 98: 141-149

[60] Ohashi S, Iemura T, Okada N, Itoh S, Furukawa H, Okuda M, Ohnishi-Kameyama M, Ogawa T, Miyashita H, Watanabe T, Itoh S, Oh-oka H, Inoue K and Kobayashi M (2010) An overview on

[61] chlorophylls and quinones in the photosystem I-type reaction centers. Photosynth. Res.104: 305-319

[62] Ohkubo S, Usui H and Miyashita H (2011) Unique chromatic adaptation of a unicellular cyanobacterium newly isolated from Lake Biwa. Jpn. J. Phycol. (Sorui) 59: 52(A22) (in Japanese)

[63] Parson WW, Clayton RK and Cogdell RJ (1975) Excited states of photosynthetic reaction centers at low redox potentials. Biochim Biophys Acta 387: 265-278

[64] Pelletier PJ and Caventou JB (1818) Ann. Chim. Phys. 9: 194

[65] Petke JD, Maggiora G, Shipman L and Christoffersen R (1979) Stereoelectronic Properties of Photosynthetic and related systems - v. ab initio configuration interaction calculations on the ground and lower excited singlet and triplet states of ethyl chlorophyllide a and ethyl pheophorbide a. Photochem.Photobiol. 30: 203-223.

[66] Porra RJ and Scheer H (2000) 18O and mass spectrometry in chlorophyll research: Derivation and loss of oxygen atoms at the periphery of the chlorophyll macrocycle during biosynthesis, degradation and adaptation. Photosynth. Res. 66: 159–175

[67] Rockley MG, Windsor MW, Cogdell RJ and Parson WW (1975) Picosecond detection of an intermediate in the photochemical reaction of bacterial photosynthesis. Proc. Natl. Acad. Sci. USA 72: 2251-2255

[68] Schoch S (1978) The esterification of chlorophyllide a in greening bean leaves. Z . Naturforsch., C: Biosci. 33C: 712-714.

[69] Shoaf W T (1978) Rapid method for the separation of chlorophylls a and b by high-pressure liquid chromatography. J. Chromatogr. 152: 247-249.

[70] Shuvalov VA, Amesz J and Duysens LNM (1986a) Picosecond spectroscopy of isolated membranes of the photosynthetic green sulfur bacterium Prosthecochloris aestuarii upon selective excitation of the primary electron donor. Biochim. Biophys. Acta 851: 1-5

[71] Shuvalov VA, Vasmel H, Amesz J and Duysens LNM (1986b) Picosecond spectroscopy of the charge separation in reaction centers of Chloroflexus aurantiacus with selective excitation of the primary electron donor. Biochim. Biophys. Acta 851: 361-368

[72] Sivakumar V, Wang R and Hastings G (2003) Photo-oxidation of P740, the primary electron donor in photosystem I from Acaryochloris marina. Biophys. J. 85:3162–3172

[73] Smith KM (1975) Mass spectrometry of porphyrins and metalloporphyrins. In: Smith KM (ed) Porphyrins and Metalloporphyrins, pp 381-398, Elsevier Scientific Publishing Company, Amsterdam

[74] Smith KM and Unsworth JM (1975) The nuclear magnetic resonance spectra of porphyrins-⊚1. Tetrahedon 31: 367-375

[75] Strain HH and Manning WM (1942) Isomerization of chlorophylls a and b. J. Biol. Chem. 146: 275-276

[76] Swingley WD, Chen M, Cheung PC, Conrad AL, Dejesa LC, Hao J, Honchak BM, Karbach LE, Kurdoglu A, Lahiri S, Mastrian SD, Miyashita H, Page L, Ramakrishna P, Satoh S, Sattley WM, Shimada Y, Taylor HL, Tomo T, Tsuchiya T, Wang ZT, Raymond J, Mimuro M, Blankenship RE and Touchman JW (2008) Niche adaptation and genome expansion in the chlorophyll d-producing cyanobacterium Acaryochloris marina. Proc. Natl. Acad. Sci .USA 105:2005–2010.

[77] Telfer A, Pascal A, Barber J, Schenderlein M, Schlodder E and Çetin M (2007) Electron transfer reactions in photosystem I and II of the chlorophyll d containing cyanobacterium, Acaryochloris marina. Photosynth. Res. 91:143

[78] Tomitani A, Okada K, Miyashita H, Matthijs HCP, Ohno T and Tanaka T (1999) Chlorophyll b and phycobilins in the common ancestor of cyanobacteria and chloroplasts. Nature 400: 159-162.

[79] Tomo T, Okubo T, Akimoto A, Yokono M, Miyashita H, Tsuchiya T, Noguchi T and Mimuro M (2007) Identification of the special pair of photosystem II in a chlorophyll d-dominated cyanobacterium. Proc. Natl. Acad. Sci. USA 104: 7283-7288

[80] Tomo T, Kato Y, Suzuki T, Akimoto S, Okubo T, Noguchi T, Hasegawa K, Tsuchiya T, Tanaka K, Fukuya M, Dohmae N, Watanabe T and Mimuro M (2008) Characterization of highly purified photosystem I complexes from the chlorophyll d-dominated cyanobacterium Acaryochloris marina MBIC 11017. J. Biol. Chem. 283:18198-18209

[81] van Gorkom HJ (1974) Identification of the reduces primary electron acceptor of photosystem II as a bound semiquinone anion. Biochim. Biophys. Acta 347: 439-442

[82] Wasielewski MR, Smith RL and Kostka AG (1980) Electrochemical production of chlorophyll a and pheophytin a excited states. J. Am. Chem. Soc. 102: 6923-6928.

[83] Watanabe T, Hongu A, Honda K, Nakazato M, Konno M and Saitoh S (1984) Preparation of chlorophylls and pheophytins by isocratic liquid chromatography. Anal. Chem. 56: 251-256

[84] Watanabe T, Nakazato M, Konno M, Saitoh S and Honda K (1984) Epimerization in the pheophytin a/a' system. Chem. Lett. 1411-1414

[85] Watanabe T and Kobayashi M (1991) Electrochemistry of chlorophylls, in: H. Scheer(ed.), Chlorophylls, CRC Press, Boca Raton pp. 287–315.

[86] Weiss C (1978) Electronic absorption spectra of chlorophylls. In: Dolphin D (ed) The Porphyrins, Vol. III, Physical Chemistry, Part A, pp 211-223. Academic Press, New York

[87] Wolf H and Scheer H (1973) Stereochemistry and chiroptic properties of pheophorbides and related compounds. Ann. N. Y. Acad. Sci. 206: 549-567

[88] Zouni A, Witt HT, Kern J, Fromme P, KrauβN, Saenger W and Orth P (2001) Crystal structure of photosystem II from Synechococcus elongatus at 3.8 Å resolution. Nature 409: 739-743